JGR Atmospheres

RESEARCH ARTICLE
10.1029/2022JD036937

A Global-Scale Mineral Dust Equation

Xuan Liu[1], Jay R. Turner[1], Jenny L. Hand[2], Bret A. Schichtel[3], and Randall V. Martin[1]

[1]Department of Energy, Environmental and Chemical Engineering, Washington University in St. Louis, St. Louis, MO, USA, [2]Cooperative Institute for Research in the Atmosphere, Colorado State University, Fort Collins, CO, USA, [3]Air Resources Division, National Park Service, Lakewood, CO, USA

Key Points:

- A global-scale mineral dust equation with region-specific coefficients is developed to estimate dust mass
- The global equation reduced regional biases by about 6%–10% compared to the Interagency Monitoring of Protected Visual Environments equation for desert dust in source regions
- Flexible options are developed to expand the global equation for special types of dust containing adsorbed water and salt minerals

Supporting Information:

Supporting Information may be found in the online version of this article.

Correspondence to:

R. V. Martin and J. R. Turner,
rvmartin@wustl.edu;
jrturner@wustl.edu

Citation:

Liu, X., Turner, J. R., Hand, J. L., Schichtel, B. A., & Martin, R. V. (2022). A global-scale mineral dust equation. *Journal of Geophysical Research: Atmospheres*, *127*, e2022JD036937. https://doi.org/10.1029/2022JD036937

Received 15 APR 2022
Accepted 3 SEP 2022

Abstract A robust method to estimate mineral dust mass in ambient particulate matter (PM) is essential, as the dust fraction cannot be directly measured but is needed to understand dust impacts on the environment and human health. In this study, a global-scale dust equation is developed that builds on the widely used Interagency Monitoring of Protected Visual Environments (IMPROVE) network's "soil" formula that is based on five measured elements (Al, Si, Ca, Fe, and Ti). We incorporate K, Mg, and Na into the equation using the mineral-to-aluminum (MAL) mass ratio of $(K_2O + MgO + Na_2O)/Al_2O_3$ and apply a correction factor (CF) to account for other missing compounds. We obtain region-specific MAL ratios and CFs by investigating the variation in dust composition across desert regions. To calculate reference dust mass for equation evaluation, we use total-mineral-mass (summing all oxides of crustal elements) and residual-mass (subtracting non-dust species from total PM) approaches. For desert dust in source regions, the normalized mean bias (NMB) of the global equation (within ±1%) is significantly smaller than the NMB of the IMPROVE equation (−6% to 10%). For $PM_{2.5}$ with high dust content measured by the IMPROVE network, the global equation estimates dust mass well (NMB within ±5%) at most sites. For desert dust transported to non-source regions, the global equation still performs well (NMB within ±2%). The global equation can also represent paved road, unpaved road, and agricultural soil dust (NMB within ±5%). This global equation provides a promising approach for calculating dust mass based on elemental analysis of dust.

1. Introduction

Mineral dust, also referred to as soil (Malm et al., 1994), geological minerals (Chow et al., 2015), and crustal material (Snider et al., 2016), is commonly defined as airborne minerals originating from soil, and is a major component of ambient particulate matter (PM) including $PM_{2.5}$ (aerodynamic diameter <2.5 μm) and PM_{10} (aerodynamic diameter <10 μm). Mineral dust has both natural (e.g., desert) and anthropogenic (e.g., agricultural soil, roads, and industry) sources, affecting visibility (e.g., Ashley et al., 2015; Hand et al., 2014, 2020; Kavouras et al., 2009), human health (e.g., Goudie, 2014; Tong et al., 2017; X. Zhang et al., 2016), the climate system (e.g., Miller & Tegen, 1998; Sokolik et al., 2001; Tegen, 2003), and biogeochemistry (e.g., Jickells et al., 2005; Koren et al., 2006; N. M. Mahowald et al., 2010; Muhs et al., 2012). The dust mass and therefore the dust fraction in PM cannot be measured directly because mineral dust is a complex mixture of many minerals, majorly quartz, feldspars, clays, calcite, and iron oxides (e.g., Nowak et al., 2018), and is often mixed with non-dust PM species that also contain crustal elements (e.g., Deboudt et al., 2010; Li et al., 2014). The practical and typical way to estimate dust mass is by applying a dust equation to sum oxides of major crustal elements by using measured elemental composition and assuming common oxide forms associated with dust. An accurate dust equation is essential to estimate the dust contribution to measured aerosols (e.g., Andrews et al., 2000; Chow et al., 2015; Malm et al., 1994; Snider et al., 2016), and to serve as a reference to evaluate and improve atmospheric models (e.g., Appel et al., 2013; Kok et al., 2021; L. Zhang et al., 2013) and satellite remote sensing algorithms (e.g., Diner et al., 2018).

Table 1 summarizes dust equations used in previous studies and various sources of error. Most dust equations omit some important dust components such as carbonate. The calcite ($CaCO_3$) content of dust can exceed 20 weight percent (wt%) in some deserts such as the Sahara (e.g., Scheuvens et al., 2013) and the Middle East (e.g., Ahmady-Birgani et al., 2015; Awadh, 2012). Thus, neglecting carbonate when estimating dust mass for these areas can cause substantial errors. Some dust equations (e.g., Andrews et al., 2000; Hueglin et al., 2005; Pryor et al., 1997) include K or Mg directly into the equation without excluding the non-dust component of these elements such as K from biomass burning and Mg from sea salt, which will therefore overestimate dust K or Mg.

Table 1
Summary of Dust Equations Used in Previous Studies

Reference	Dust equation	Sources of error
(Macias & Hopke, 1981)	1.89Al + 2.14Si + 1.4Ca + 1.43Fe + 1.2K	Missing carbonate, oxides of Na, Mg, Ti, etc.; K susceptible to biomass burning
(Chow et al., 1994; Solomon et al., 1989)	1.89Al + 2.14Si + 1.4Ca + 1.43Fe	Missing carbonate, oxides of Na, Mg, K, Ti, etc.
(Malm et al., 1994)	[1.89Al + 2.14Si + 1.40Ca + (1.36 + 0.6 × 1.20) Fe + 1.67Ti] × 1.16 = 2.20Al + 2.49Si + 1.63Ca + 2.42Fe + 1.94Ti (**IMPROVE**)	Accuracy of the correction factor for missing compounds; Developed for the U.S.
(Pryor et al., 1997)	2.2Al + 2.49Si + 1.63Ca + 1.5Fe + 1.4K + 1.94Ti	Accuracy of the correction factor for missing compounds; K susceptible to biomass burning
(Andrews et al., 2000; Kleindienst et al., 2010)	1.89Al + 2.14Si + 1.4Ca + 1.43Fe + 1.67Ti + 1.2K	Missing carbonate, oxides of Na, Mg, etc.; K susceptible to biomass burning
(Hueglin et al., 2005)	1.89Al + 2.14Si + 1.40Ca + 1.43Fe + 1.21K + 1.66Mg	Missing carbonate, oxides of Na, Ti, etc.; K susceptible to biomass burning; Mg susceptible to sea salt
(Terzi et al., 2010)	1.89Al + 2.14Si + 1.95Ca + 1.43Fe + 1.67Ti + 1.2K + 1.66Mg	Missing carbonate, oxides of Na, etc.; K susceptible to biomass burning; Mg susceptible to sea salt
(Ni et al., 2013)	1.89Al + 2.14Si + 1.40Ca + 1.43Fe + 1.67Ti + 1.21K + 1.66Mg	Missing carbonate, oxides of Na, etc.; K susceptible to biomass burning; Mg susceptible to sea salt

The U.S. Interagency Monitoring of Protected Visual Environments (IMPROVE) network's "soil" formula (Soil = 2.20Al + 2.49Si + 1.63Ca + 2.42Fe + 1.94Ti) was developed to characterize mineral dust within the United States (Malm et al., 1994), but is used worldwide. The IMPROVE equation assumes that iron is split equally between Fe_2O_3 and FeO in soil according to their abundance in most rock types (Eldred, 2003). Soil K is incorporated as a fraction (0.6) of Fe to avoid the influence of smoke K emitted by biomass burning (Eldred, 2003; Pachon et al., 2013). A correction factor (CF) of 1.16 is applied to all five elements to account for other missing compounds (mainly MgO, Na_2O, CO_2, and H_2O) based on the composition of average sediment (Eldred, 2003; Pettijohn, 1975). Across the IMPROVE network, the elemental composition of $PM_{2.5}$ samples is measured using X-ray fluorescence (XRF) and the above equation is applied to estimate soil (dust) mass. Although the IMPROVE equation is designed to address many of the challenges associated with dust characterization, Malm and Hand (2007) found that dust mass across the IMPROVE network may be underestimated by ∼20%, suggesting that the IMPROVE equation needs further development.

Several issues need to be addressed to further develop the IMPROVE equation for mineral dust on a global scale. First, the relationship between soil K and Fe may change in regions outside the US or even within the US because of the variation in dust composition (e.g., Journet et al., 2014). Second, although using Fe as a surrogate for soil K works well for natural dust at IMPROVE sites, for anthropogenic dust in urban areas, Al or Si should be a better choice than Fe given that the Fe concentration is more likely affected by non-dust sources such as combustion (e.g., Chen et al., 2012). Third, the fraction of missing compounds in dust may also differ inside or outside the US. Fourth, the data of average sediment (Pettijohn, 1975) used to derive the factor of 1.16 might not represent natural dust composition which is usually represented using the data of continental crust from other sources (e.g., Cao et al., 2008; Choi et al., 2001; Contini et al., 2010; Ganor et al., 1991; Gao et al., 2018; Radhi et al., 2010a). Fifth, liquid water (different from crystal water) associated with special types of dust can be non-negligible. Dust is commonly assumed to be non-hygroscopic, but high hygroscopicity has been observed for saline dust in some regions (e.g., Gaston, 2020; Gaston et al., 2017; Koehler et al., 2007; Tang et al., 2019), some types of aged dust (e.g., Sullivan et al., 2009; Tang et al., 2016), and some types of anthropogenic dust (e.g., Peng et al., 2020). Sixth, special types of dust such as saline dust (e.g., Gaston et al., 2017), volcanic dust (e.g., Gislason et al., 2011; Taylor & Lichte, 1980), and aged dust (e.g., Tang et al., 2016) may contain salt minerals that are not considered for common desert dust. Some studies have applied the IMPROVE equation to natural or anthropogenic dust

measured outside the US (e.g., Ho et al., 2003; K. W. Kim et al., 2001; Matawle et al., 2015; Pant et al., 2015; Z. X. Shen et al., 2007; Wu et al., 2011), yet to our knowledge, none have demonstrated its accuracy for that purpose. The development of a global-scale dust equation should address the issues discussed above and assess its performance both within and outside the US.

In this study, we develop a global-scale dust equation that builds upon the IMPROVE "soil" formula using analyses of the elemental composition and carbonate content of desert dust in different regions compared with that of continental crust. The global equation is evaluated for desert dust over source/non-source regions, dust in the U.S. IMPROVE monitoring network, and major types of anthropogenic dust. The performance of the IMPROVE equation is treated as a well-respected benchmark to evaluate the global equation. The goal of this study is to develop a global dust equation with regional parameterization that reduces the regional bias in dust mass estimated using measured elemental data. The reduced bias is especially important to PM mass closure (e.g., Ni et al., 2013; Terzi et al., 2010) and model evaluation (e.g., Appel et al., 2013; Meng et al., 2021; L. Zhang et al., 2013).

2. Data and Methods

2.1. Development of the Global Dust Equation

The five major crustal elements (Al, Si, Ca, Fe, and Ti) of the IMPROVE equation were used in the global equation assuming common oxide forms of Al_2O_3, SiO_2, CaO, FeO, and Fe_2O_3 (in equal amounts), and TiO_2, respectively. However, in contrast to the use of Fe in the IMPROVE equation to estimate soil K, Al was investigated as the new surrogate and used to estimate dust components of K, Mg, and Na by defining a mineral-to-aluminum (MAL) mass ratio as $(K_2O + MgO + Na_2O)/Al_2O_3$. We combined these three elements into one coefficient because they are all major crustal elements that cannot be directly included due to their potentially significant sources from biomass burning and sea salt. We included only dust components of these elements by applying the MAL ratio obtained using dust data with negligible non-dust sources. The MAL ratio can be converted to:

$$\mathrm{MAL} = (1.20\mathrm{K}/\mathrm{Al} + 1.66\mathrm{Mg}/\mathrm{Al} + 1.35\mathrm{Na}/\mathrm{Al})/1.89 \quad (1)$$

where 1.20, 1.66, 1.35, and 1.89 are the oxide factors that convert elements to oxides for K_2O, MgO, Na_2O, and Al_2O_3, respectively. Thus, with elemental ratios of dust, the MAL ratio can be calculated and compared between regions. The MAL ratio is similar to the Chemical Index of Alteration defined as $100 \times Al_2O_3/(Al_2O_3 + CaO + Na_2O + K_2O)$ and the Weathering Index of Parker represented as $100 \times (2Na_2O/0.35 + MgO/0.9 + 2K_2O/0.25 + CaO/0.7)$ (Price & Velbel, 2003), in the sense of representing the relative abundance of alkalis in dust.

We next examined the contribution from other elements. Although according to the composition of the upper continental crust (UCC) (Shaw et al., 1986), both CO_2 (decomposed from carbonate) and the sum of remaining compounds (mainly crystal H_2O, P_2O_5, and MnO) account for 1 wt% of UCC, for mineral dust in arid areas, the CO_2 content can reach up to 10 wt% or higher (Awadh, 2012; Modaihsh, 1997; Scheuvens et al., 2013). The abundance of bound H_2O, P_2O_5, and MnO is relatively consistent with that in the UCC (N. Mahowald et al., 2008; Mendez et al., 2010; Moreno et al., 2006; Moufti, 2013; Najafi et al., 2014; Zarasvandi et al., 2011). Therefore, we further investigated the regionally resolved CO_2 content at dry conditions but fixed the abundance of remaining compounds as 1 wt%. We derived an overall CF as:

$$\mathrm{CF} = \frac{100\,\mathrm{wt}\%}{100\,\mathrm{wt}\% - [1\,\mathrm{wt}\% + \mathrm{CO_2(wt}\%)]} \quad (2)$$

Including the MAL ratio and CF, we proposed a global-scale mineral dust equation:

$$\mathrm{Dust} = [1.89\mathrm{Al} \times (1 + \mathrm{MAL}) + 2.14\mathrm{Si} + 1.40\mathrm{Ca} + 1.36\mathrm{Fe} + 1.67\mathrm{Ti}] \times \mathrm{CF} \quad (3)$$

where 1.89, 2.14, 1.40, 1.36, and 1.67 are the oxide factors for Al_2O_3, SiO_2, CaO, FeO, and Fe_2O_3 (in equal amounts), and TiO_2, respectively. Both the MAL ratio and CF vary regionally. Because the MAL ratio is estimated using dust data with negligible non-dust sources, the dust mass calculated by the global equation will exclude non-dust components of K, Mg, and Na when these elements are influenced by non-dust sources such as wildfire or sea salt. Similarly, we tested a mineral-to-silicon (MSI) ratio as $(K_2O + MgO + Na_2O)/SiO_2$ to examine the feasibility of using Si as the surrogate to estimate K, Mg, and Na.

To include adsorbed water and salt minerals for special types of dust such as saline dust, volcanic dust, and aged dust, we derived an expanded global equation with expanded MAL and CF as described in Text S1 in Supporting Information S1. A water adjustment factor (WAF) was included in the CF based on the single hygroscopicity parameter κ (Kreidenweis et al., 2008; Snider et al., 2016). Although insufficient measured data were available to calculate the coefficients in the expanded global equation for these special types of dust, the expanded equation offers a framework to represent these special cases when detailed mineralogical information and hygroscopicity measurements are available in addition to elemental data. Dust hygroscopicity κ depends on many factors including the dust mineralogy or salinity (Tang et al., 2019), chemical mixing state (Sullivan et al., 2009), emission source (Peng et al., 2020), and particle size (Ibrahim et al., 2018). A review of the literature reveals that the κ of common desert dust is low (<0.1; Gaston et al., 2017; Herich et al., 2009; Koehler et al., 2009; Tang et al., 2019), but for saline dust κ can be higher (>0.8; Gaston et al., 2017; Tang et al., 2019). For dust with high hygroscopicity, for example, $\kappa = 1.0$, the resulting WAF will be 1.2, meaning adsorbed water can reach 20 wt% of the dry dust mass. For common desert dust, K, Mg, and Na exist mainly in feldspar or illite with low hygroscopicity (Tang et al., 2019), but they can exist mostly in salt minerals with high hygroscopicity for special types of dust such as saline dust. Salt minerals commonly observed in various special types of dust require the expanded global equation. For example, saline dust can have significant amounts of chlorides and sulfates besides carbonates, such as NaCl and Na_2SO_4 (Gaston et al., 2017). Volcanic dust has non-negligible sulfates, chlorides, and fluorides, such as $MgSO_4$, NaCl, and K_2SiF_6 (Gislason et al., 2011; Taylor & Lichte, 1980). Aged dust can contain nitrates, sulfates, and chlorides, such as $Ca(NO_3)_2$, $CaSO_4$, and $CaCl_2$ (Sullivan et al., 2009).

To investigate variation in the MAL and MSI ratios of desert dust across different regions, we collected elemental characteristics data (elemental ratios) of mineral dust in six major dust source regions (Sahara, Sahel, Middle East, East Asia, Australia, and Southwest US) as shown in Table 2. Other source regions such as South Africa and South America were not selected because insufficient measured data are available for these regions. Figure S1 in Supporting Information S1 summarizes the median and interquartile range of elemental ratios and MAL for each region. The data we used were obtained from various analysis techniques such as XRF, inductively coupled plasma-mass spectrometry (ICP-MS), and particle-induced X-ray emission (PIXE). These techniques have different detection limits and analytical errors, which can generate uncertainties on the elemental ratios, an inevitable problem for compiling different published analyses (Scheuvens et al., 2013), so we used the median value to reduce the influence of outliers. For the Southwest US, we used $PM_{2.5}$ data with dust mass (SOIL) > 50% of the reconstructed fine mass (RCFM) based on the IMPROVE algorithm (http://vista.cira.colostate.edu/Improve/reconstructed-fine-mass/) measured at IMPROVE rural sites. The measured data in other dust source regions were collected from literature and the Surface Particulate Matter Network (SPARTAN, Snider et al., 2015, https://www.spartan-network.org/). Given that Na and Mg potentially come from sea salt and K from biomass burning, to ensure negligible non-dust sources of Na, Mg, and K in the collected dust data from literature, we excluded the data affected by sea salt or biomass burning indicated by the dust origin analysis in their literature sources, which removed ~20 potential data sources. We incorporated different types of dust (aerosol, soil, and sediment) to augment the data set size. We neglected the difference in elemental ratios between different types of dust because insufficient previous studies are available to examine this concern. As a reference, the MAL and MSI ratios for average continental crust were calculated using elemental ratios from commonly cited sources for natural dust (Lide, 1995; Mason, 1952; Taylor & McLennan, 1995; Wedepohl, 1995). We applied the Kruskal-Wallis test to compare the MAL and MSI ratios in major dust source regions and continental crust. The criterion of a calculated probability with significance level <0.05 ($P < 0.05$) was used as a measure of statistically significant differences between the groups. When the measurements of any element used in the global equation are not available or not well characterized, the median elemental ratios for each region shown in Table 2 could be applied to estimate the concentration of that element.

Measurements of the CO_2 content in dust are commonly omitted, which handicaps the investigation of its regional variability. Thus, an indirect way to estimate CO_2 content is needed. We obtained the worldwide distribution of $CaCO_3$ content in topsoil (0–30 cm) from the Harmonized World Soil Database (HWSD version 1.21, FAO & ISRIC, 2012). This distribution is generally consistent with the mineralogical maps from several modeling studies (Claquin et al., 1999; Journet et al., 2014; Nickovic et al., 2012). We estimated the average $CaCO_3$ content in major dust source regions using an embedded query Tool in the HWSD viewer. We also used mineralogical maps for carbonates in the topsoil (A horizon, 5–10 cm) of the conterminous US from the U.S. Geological Survey (USGS, Smith et al., 2019) as a reference. To account for other carbonates in dust, we calculated the mass ratio

Table 2
Elemental Ratios of Dust in Major Dust Source Regions and Continental Crust

Region	Site	Type	Size (μm)	Si/Al	Fe/Al	Ca/Al	Ti/Al	K/Al	Mg/Al	Na/Al	MAL	K/Fe	Source	Method
Crust	Upper continental crust	Rock		3.83	0.44	0.37	0.04	0.35	0.17	0.36	0.63	0.80	(Taylor & McLennan, 1995)	NA
	Upper continental crust	Rock		3.92	0.40	0.38	0.04	0.33	0.17	0.33	0.60	0.83	(Wedepohl, 1995)	NA
	Continental crust	Rock		3.41	0.62	0.45	0.05	0.32	0.26	0.35	0.68	0.52	(Lide, 1995)	NA
	Continental crust	Rock		3.43	0.68	0.50	0.07	0.25	0.28	0.29	0.61	0.37	(Mason, 1952)	NA
	Median			**3.63**	**0.53**	**0.42**	**0.05**	**0.33**	**0.22**	**0.34**	**0.62**	**0.66**		
Middle East	Southwest Iran	Aerosol	0.8–50	NA	NA	1.15	0.08	0.22	0.29	0.13	0.49	NA	(Torghabeh et al., 2020)	ICP-OES
	Western Iran	Aerosol	TSP	3.57	0.66	2.86	0.07	0.23	0.56	0.11	0.72	0.35	(Najafi et al., 2014)	XRF
	Central Iran 2008	Aerosol	TSP	4.34	0.79	4.28	0.10	0.22	0.44	0.21	0.68	0.29	(Hojati et al., 2012)	ICP-MS
	Central Iran 2009	Aerosol	TSP	3.29	0.76	5.36	0.14	0.22	0.46	0.32	0.78	0.29	(Hojati et al., 2012)	ICP-MS
	Ahvaz, Iran 2009	Aerosol	TSP	NA	1.14	4.73	0.02	0.32	0.89	0.21	1.14	0.28	(Zarasvandi et al., 2011)	ICP-MS
	Israel[a]	Aerosol	$PM_{2.5}$	2.71	0.61	0.68	0.06	0.37	0.21	0.37	0.68	0.60		XRF
	Abu Dhabi[a]	Aerosol	$PM_{2.5}$	3.05	0.76	2.03	0.06	0.38	0.70	0.23	1.02	0.50		XRF
	Median			**3.29**	**0.76**	**2.86**	**0.07**	**0.23**	**0.46**	**0.21**	**0.72**	**0.32**		
Sahara	Northern Algeria	Aerosol	0.1–1	1.85	0.45	1.09	0.06	0.17	NA	NA	NA	0.38	(Gomes et al., 1990)	XRF
	Northern Algeria	Aerosol	1–20	2.12	0.48	0.88	0.06	0.19	NA	NA	NA	0.40	(Gomes et al., 1990)	XRF
	Morocco	Aerosol	TSP	4.97	0.64	5.22	0.09	0.40	0.86	NA	NA	0.63	(Khiri et al., 2004)	XRF
	Khamaseen dust	Aerosol	5–20	4.05	0.73	3.60	0.13	0.25	0.58	0.13	0.77	0.33	(Abed et al., 2009)	ICP-MS
	Cairo	Aerosol	<20	5.83	0.70	2.00	0.14	0.28	0.57	0.16	0.80	0.40	(Linke et al., 2006)	XRF
	Cairo	Soil	<20	6.33	0.77	4.26	0.21	0.24	0.43	0.20	0.67	0.31	(Linke et al., 2006)	XRF
	Morocco	Soil	<20	7.41	0.57	1.85	0.11	0.38	0.31	0.09	0.58	0.66	(Linke et al., 2006)	XRF
	Western Sahara site 1	Soil	<30	6.26	0.66	1.98	0.08	0.34	0.37	0.15	0.66	0.52	(Moreno et al., 2006)	ICP-AES
	Western Sahara site 2	Soil	<30	5.82	0.53	3.40	0.07	0.37	0.42	0.15	0.71	0.70	(Moreno et al., 2006)	ICP-AES
	Western Sahara site 3	Soil	<30	9.88	1.10	3.24	0.20	0.42	0.43	0.23	0.80	0.38	(Moreno et al., 2006)	ICP-AES
	Hoggar Massif site 1	Soil	<30	3.72	0.54	0.22	0.11	0.26	0.14	0.15	0.40	0.48	(Moreno et al., 2006)	ICP-AES
	Hoggar Massif site 2	Soil	<30	4.06	0.50	0.20	0.10	0.28	0.13	0.20	0.44	0.56	(Moreno et al., 2006)	ICP-AES
	Tindouf, Algeria	Soil	<63	4.68	0.65	6.52	0.11	0.34	0.96	0.48	1.40	0.52	(Criado & Dorta, 2003)	ICP-AES
	Tiris, Mauritania	Soil	<63	7.07	0.53	0.25	0.17	0.42	0.14	0.20	0.53	0.79	(Criado & Dorta, 2003)	ICP-AES
	Northern Mali	Soil	NA	NA	0.49	7.95	NA	0.27	0.65	0.13	0.84	0.57	(Washington et al., 2009)	NA
	Median			**5.40**	**0.57**	**2.00**	**0.11**	**0.28**	**0.43**	**0.16**	**0.69**	**0.52**		
Sahel	Dakar, Senegal	Aerosol	TSP	5.62	0.62	0.25	0.09	0.24	0.15	0.09	0.35	0.38	(Orange et al., 1993)	NA
	Mbour, Senegal	Aerosol	TSP	6.69	0.68	0.14	0.10	0.16	0.16	0.02	0.26	0.24	(Orange et al., 1993)	NA
	Pete, Senegal	Aerosol	TSP	6.59	0.67	0.12	0.10	0.16	0.15	0.01	0.24	0.25	(Orange et al., 1993)	NA
	Zaria, Northern Nigeria	Aerosol	<2	2.23	0.42	0.01	0.06	0.10	0.09	0.00	0.14	0.23	(Møberg et al., 1991)	AAS

Table 2
Continued

Region	Site	Type	Size (μm)	Si/Al	Fe/Al	Ca/Al	Ti/Al	K/Al	Mg/Al	Na/Al	MAL	K/Fe	Source	Method
	Niger, local	Aerosol	<40	2.50	0.57	0.21	0.11	0.17	0.10	0.04	0.22	0.29	(Formenti et al., 2008)	XRF
	Niger, advected	Aerosol	<40	2.84	0.57	0.39	0.07	0.18	0.16	0.06	0.30	0.32	(Formenti et al., 2008)	XRF
	Agadez, Niger	Soil	<20	6.10	0.23	0.08	0.03	0.49	0.04	0.27	0.54	2.13	(Linke et al., 2006)	XRF
	Niger, Monsoon	Aerosol	<30	5.29	0.50	0.04	0.13	0.16	0.05	0.04	0.17	0.32	(Moreno et al., 2006)	ICP-AES
	Niger, Harmattan	Aerosol	<30	4.84	0.62	0.18	0.11	0.23	0.08	0.07	0.27	0.37	(Moreno et al., 2006)	ICP-AES
	Chad Basin	Soil	<30	4.00	0.63	0.13	0.08	0.16	0.10	0.11	0.27	0.26	(Moreno et al., 2006)	ICP-AES
	Bodélé, Chad	Soil	NA	NA	0.64	0.04	NA	0.16	0.08	0.26	0.36	0.26	(Washington et al., 2009)	NA
	Median			**5.07**	**0.62**	**0.13**	**0.09**	**0.16**	**0.10**	**0.06**	**0.27**	**0.29**		
Australia	Birdsville, Queensland	Aerosol	TSP	3.42	0.77	0.11	0.09	0.19	NA	0.24	NA	0.24	(Radhi et al., 2010a)	PIXE, PIGE
	Muloorina station	Aerosol	TSP	3.16	0.96	0.58	0.08	0.26	NA	0.12	NA	0.27	(Radhi et al., 2010b)	PIXE, PIGE
	Ormiston creek site 1	Soil	PM_{10}	NA	0.47	0.09	0.04	0.24	0.10	0.06	0.28	0.51	(Moreno et al., 2009)	ICP-AES
	Ormiston creek site 2	Soil	PM_{10}	NA	0.44	0.05	0.04	0.17	0.05	0.05	0.19	0.40	(Moreno et al., 2009)	ICP-AES
	Wilpena pound site 1	Soil	PM_{10}	NA	0.62	0.03	0.05	0.11	0.05	0.01	0.13	0.18	(Moreno et al., 2009)	ICP-AES
	Wilpena pound site 2	Soil	PM_{10}	NA	0.26	0.03	0.08	0.26	0.07	0.03	0.25	0.99	(Moreno et al., 2009)	ICP-AES
	Silverton	Soil	PM_{10}	NA	0.53	0.12	0.04	0.28	0.10	0.03	0.29	0.53	(Moreno et al., 2009)	ICP-AES
	Queensland	Sediment	<80	3.45	0.59	0.09	0.09	0.14	0.10	0.06	0.23	0.23	(Kamber et al., 2005)	ICP-OES
	Autralian continent	Sediment	<2, 000	8.47	0.53	0.08	0.08	0.23	0.07	0.05	0.25	0.44	(Reimann & de Caritat, 2012)	XRF
	Median			**3.44**	**0.53**	**0.09**	**0.08**	**0.23**	**0.07**	**0.05**	**0.25**	**0.40**		
East Asia	Zhenbeitai, China	Aerosol	TSP	4.14	0.52	0.79	0.08	0.25	0.26	NA	NA	0.48	(X. Y. Zhang et al., 2003)	PIXE
	Zhenbeitai, China	Aerosol	PM_9	2.79	0.63	0.79	0.05	0.31	0.32	0.19	0.62	0.49	(Alfaro, 2003)	XRF
	Zhenbeitai, China	Aerosol	$PM_{2.5}$	1.90	0.59	1.00	0.05	0.32	0.35	0.15	0.62	0.54	(Arimoto, 2004)	PIXE
	Yulin, China	Aerosol	$PM_{2.5}$	NA	0.51	0.81	0.07	0.46	0.24	0.19	0.64	0.90	(Xu, 2004)	ICP-MS
	Gansu, China	Aerosol	TSP	2.94	0.35	0.74	0.03	0.27	0.31	0.11	0.52	0.77	(Ta et al., 2003)	XRF
	Desert area, China	Soil	<100	7.68	0.54	0.94	0.06	0.34	0.28	0.29	0.68	0.63	(Ta et al., 2003)	XRF
	Gobi area, China	Soil	<100	7.85	0.35	1.17	0.04	0.39	0.18	0.36	0.67	1.09	(Ta et al., 2003)	XRF
	Gansu, China	Soil	<30	4.61	0.49	0.97	0.06	0.32	0.26	0.22	0.59	0.66	(Nishikawa et al., 2000)	XRF, etc.[b]
	Ningxia, China	Soil	<30	4.76	0.51	0.91	0.08	0.29	0.27	0.23	0.59	0.56	(Nishikawa et al., 2000)	XRF, etc.
	Xi Feng, China	Soil	TSP	4.56	0.78	2.25	0.07	0.41	0.28	0.06	0.55	0.52	(Wu et al., 2011)	XRF
	Xi Feng, China	Soil	PM_{10}	2.03	0.71	2.30	0.06	0.39	0.29	0.08	0.56	0.55	(Wu et al., 2011)	XRF
	Xi Feng, China	Soil	$PM_{2.5}$	1.78	0.65	1.56	0.05	0.29	0.29	0.07	0.49	0.44	(Wu et al., 2011)	XRF
	Xi Feng, China	Soil	PM_1	1.88	0.68	1.77	0.05	0.29	0.29	0.06	0.49	0.43	(Wu et al., 2011)	XRF
	Median			**3.54**	**0.54**	**0.97**	**0.06**	**0.32**	**0.28**	**0.17**	**0.59**	**0.55**		

Table 2
Continued

Region	Site	Type	Size (μm)	Si/Al	Fe/Al	Ca/Al	Ti/Al	K/Al	Mg/Al	Na/Al	MAL	K/Fe	Source	Method
Southwest US[c]	Jarbidge wilderness	Aerosol	$PM_{2.5}$	2.86	0.60	0.49	0.05	0.43	0.25	0.30	0.71	0.71		XRF
	Saguaro NM	Aerosol	$PM_{2.5}$	2.33	0.58	0.68	0.05	0.36	0.22	0.24	0.59	0.61		XRF
	Meadview	Aerosol	$PM_{2.5}$	2.40	0.63	0.78	0.06	0.36	0.30	0.26	0.68	0.57		XRF
	Owens valley	Aerosol	$PM_{2.5}$	2.50	0.60	0.78	0.05	0.38	0.37	0.27	0.76	0.64		XRF
	Tonto NM	Aerosol	$PM_{2.5}$	2.32	0.58	0.63	0.05	0.34	0.26	0.24	0.62	0.59		XRF
	Chiricahua NM	Aerosol	$PM_{2.5}$	2.36	0.53	0.63	0.05	0.35	0.20	0.27	0.59	0.65		XRF
	Petrified forest NP	Aerosol	$PM_{2.5}$	2.31	0.60	0.71	0.05	0.32	0.27	0.20	0.58	0.54		XRF
	Canyonlands NP	Aerosol	$PM_{2.5}$	2.31	0.56	0.88	0.05	0.36	0.32	0.19	0.65	0.65		XRF
	White mountain	Aerosol	$PM_{2.5}$	2.40	0.57	1.10	0.05	0.33	0.42	0.21	0.73	0.58		XRF
	Capitol reef NP	Aerosol	$PM_{2.5}$	2.48	0.63	1.02	0.06	0.39	0.38	0.22	0.74	0.62		XRF
	Zion canyon	Aerosol	$PM_{2.5}$	2.44	0.60	1.01	0.06	0.37	0.40	0.27	0.77	0.61		XRF
	Gila wilderness	Aerosol	$PM_{2.5}$	2.29	0.55	0.78	0.05	0.34	0.26	0.18	0.58	0.62		XRF
	Median			**2.38**	**0.59**	**0.78**	**0.05**	**0.36**	**0.29**	**0.24**	**0.66**	**0.61**		

Note. NA: not available; XRF: X-ray fluorescence; AAS: atomic absorption spectrometry; ICP-MS: inductively coupled plasma-mass spectrometry; ICP-OES: inductively coupled plasma-optical emission spectrometry; ICP-AES: inductively coupled plasma-atomic emission spectrometry; PIXE: particle-induced X-ray emission; PIGE: particle-induced gamma emission; TSP: total suspended particulate; NM: national monument; NP: national park.

[a]The Israel and UAE data are the ratios of mean element concentrations using $PM_{2.5}$ data in 2019 from the SPARTAN network. Only the data with Na/Al < 0.45 and K/Al < 0.5 were selected to avoid the effects of non-dust sources (Scheuvens et al., 2013). [b]This is a reference material certified using multiple techniques. [c]The Southwest US data are the ratios of mean element concentrations calculated using dust-dominated (SOIL > 50% RCFM) $PM_{2.5}$ data in 2011–2018 from the IMPROVE network.

of total CO_2 to the CO_2 in $CaCO_3$ using available measured mineralogical data for major deserts worldwide from literature (Boose et al., 2016; Engelbrecht et al., 2016; Z. Shen et al., 2009). Using the inferred total CO_2 abundance and fixing the remaining compounds as 1 wt%, we calculated the corresponding CF in the global equation.

The measured data assembled from the literature for this study include various sizes of dust. Because the chemical composition of dust can be size-dependent (Cao et al., 2008; Pettijohn, 1975; Z. X. Shen et al., 2007; Wu et al., 2011; Zarasvandi et al., 2011), we compared the differences of the elemental characteristics and carbonate content between PM_{10} and $PM_{2.5}$ using a data set of surface soil from arid regions (Engelbrecht et al., 2016). Detailed information on data processing is provided in Text S2 in Supporting Information S1.

In addition to employing multiple major crustal elements to estimate dust mass, single crustal elements such as Si have also been used previously (Chow et al., 2015). As a comparison, Si alone with a coefficient M (Dust = Si × M) to account for all the major minerals was also investigated by calculating the coefficient M across dust source regions.

2.2. Reference Dust Mass

To evaluate the performance of the global dust equation, we applied two approximate methods to obtain the reference dust mass since no absolute benchmark is available. One is called the total-mineral-mass approach, which is calculated by summing all the oxides of measured major crustal elements (Si, Al, Fe, Ca, Ti, Na, Mg, and K). Elemental concentrations were multiplied by corresponding common oxide factors (Reff et al., 2009) to obtain oxide concentrations. Measurements of Na, Mg, and K can be directly used to calculate dust mass only when they have negligible non-dust sources. Other dust components such as H_2O and carbonate are not commonly measured, so we applied the same CF used in the global equation to obtain "total mineral mass." The other method is the residual-mass approach, which is calculated by subtracting organic mass (OM), elemental carbon, sulfate, nitrate, ammonium, sea salt, and particle-bound water (PBW) from the measured PM. OM was calculated by multiplying OC with spatiotemporally varying estimates of the OM/OC ratio (Philip et al., 2014). Sea

salt was represented as $1.8Cl^-$, or as 1.8Cl when the Cl^- concentration was missing (Hand et al., 2012; Malm & Hand, 2007). PBW refers to water associated with sulfate, nitrate, ammonium, sea salt, and OM, which was estimated using a κ-Kohler framework (Kreidenweis et al., 2008) with specific parameters for each species at different RH conditions from Latimer and Martin (2019). Following the IMPROVE algorithm, we assumed sulfate exists as ammonium sulfate (AS) and nitrate as ammonium nitrate to calculate PBW. For anthropogenic dust such as road dust, non-dust trace metals were also subtracted because their influence on the residual mass may be non-negligible (Chow et al., 2015). Both approaches have limitations. The total-mineral-mass approach cannot directly test the accuracy of the CF because it is used in both the total mineral mass and the global equation. As for the residual-mass approach, uncertainties exist in the measurements of each PM component and related assumptions, especially the uncertainty in estimating OM (Philip et al., 2014; Simon et al., 2011). Nevertheless, both approaches offer information to evaluate our global equation. To optimize the accuracy of the reference dust mass, we used dust-dominated samples where all measurements of mineral elements were well quantified and contributions from organics and other non-dust species were negligible. The data selection and the method of calculating the reference dust mass applied for different data sources are further discussed in the next section.

To carry out the evaluation, we applied several statistical metrics including the normalized mean bias (NMB), mean fractional bias (MFB), and normalized root mean square error (NRMSE):

$$\mathrm{NMB}\,(\%) = 100 \times \sum (C_j - R_j) \,/\, \sum R_j \tag{4}$$

$$\mathrm{MFB}\,(\%) = 100 \times 1/N \times \sum (C_j - R_j) \,/\, \left[(C_j + R_j)\,/2\right] \tag{5}$$

$$\mathrm{NRMSE}\,(\%) = 100 \times 1/\sigma \times \sqrt{\sum (C_j - R_j)^2 / N} \tag{6}$$

where C_j represents the calculated dust mass, R_j is the reference dust mass obtained using the total-mineral-mass or residual-mass approach, j represents the pairing of the calculated dust mass and reference dust mass by site and time for N data points, and σ is the standard deviation of the reference dust mass. The NMB and MFB are also calculated with the IMPROVE equation to serve as a benchmark of our global equation. Some results with ratio form were plotted on a log scale so that deviations from unity are visually symmetrical.

2.3. Evaluation of the Global Dust Equation

First, we examined the performance of the global equation for desert dust in source regions and for the average global continental crust using the same data sources as those in Table 2. For the Australian dust data without Si measurements, the median Si/Al ratio (3.44) from available measurements was used. We also evaluated the global equation for desert dust (African and Asian) transported to non-source regions using measurements from the European Monitoring and Evaluation Programme (EMEP, https://www.emep.int/) and literature. We used dust data measured at southern EMEP sites during summer African dust events. To reduce the influence of sea salt and biomass burning, we selected the data with Na/Al < 0.45 and K/Al < 0.5 reflecting typical elemental ratios for Northern African dust (Scheuvens et al., 2013). After the selection, PM_{10} data from six sites during three dust episodes (Alastuey et al., 2016; Matassoni et al., 2009) were used for the evaluation. We also applied the global equation to available literature data of African dust over the Atlantic islands (Criado & Dorta, 2003; Engelbrecht et al., 2014; Formenti, 2003; Kandler et al., 2007) as well as Asian dust over Japan (Nishikawa et al., 1991) and Korea (K. H. Kim et al., 2003). We only used data with minimal influence of non-dust sources suggested in the literature. Because Si measurements were missing in the dust data over Japan and Korea, we used the median Si/Al ratio (3.54) in East Asian deserts from Table 2. For most of the above data, we were unable to apply the residual-mass approach owing to insufficient measurements of non-dust PM species, so the total-mineral-mass approach was the major method applied for the evaluation. According to the protocol of EMEP measurements, we used 50% RH to calculate PBW for EMEP data.

To further evaluate the global dust equation within the US, we utilized daily-integrated $PM_{2.5}$ speciation data from the IMPROVE network. Mineral elements are analyzed with XRF for samples from IMPROVE sites which are primarily located in rural areas (Solomon et al., 2014). Following the IMPROVE data advisories (http://vista.cira.colostate.edu/Improve/data-advisories/), we used data collected in 2011–2018 to avoid the influence of data anomalies or potential problems such as non-quantitative Na data prior to 2011 (Hyslop et al., 2015). To balance

avoiding uncertainties in the measurements of low dust content data while retaining sufficient data, we used dust-dominated $PM_{2.5}$ data (SOIL > 50% RCFM based on the IMPROVE algorithm). For cases with measured elemental concentration below the minimum detection limit (MDL), we substituted one-half of the MDL. The spatial distribution of the MAL ratio was investigated by calculating the ratio of the average $K_2O + MgO + Na_2O$ to average Al_2O_3 concentrations. The NMB and MFB for the entire data set and for each site were calculated using both total-mineral-mass and residual-mass approaches. The NRMSE was also provided for the entire data set. For the residual-mass approach, we adopted the common humidity protocol (35%) for gravimetric mass analysis to calculate PBW. Following the IMPROVE advisory about increased variation of humidity after the weighing laboratory moved in 2011, we applied an RH of 45% for summer (June–August) data after the laboratory move. The average fraction of calculated PBW in measured total $PM_{2.5}$ was ~4 wt%. All IMPROVE sites including rural and urban sites were considered but only the sites with ≥5 daily-integrated $PM_{2.5}$ records that meet the criterion of SOIL > 50% RCFM were used in our maps to ensure representativeness. We neglected the data from the U.S. National $PM_{2.5}$ Chemical Speciation Monitoring Network (CSN) given that CSN dust concentrations were inconsistent with collocated IMPROVE dust concentrations, and comparisons between the two networks would be semiquantitative (Hand et al., 2012). Gorham et al. (2021) indicated that CSN has lower flow rate and larger sample deposit area than IMPROVE which makes quantification difficult, and particle size cut point efficiency also varies between the two networks. CSN has higher MDLs for mineral elements than IMPROVE, and therefore some elements are poorly detected (e.g., Al).

We explored the applicability of the global equation for anthropogenic dust by evaluating its performance for paved road, unpaved road, and agricultural soil dust using measured $PM_{2.5}$ and PM_{10} data from the U.S. Environmental Protection Agency's (EPA) SPECIATE 5.0 database (https://www.epa.gov/air-emissions-modeling/speciate) and available data from two studies of paved road dust in Spain and China (Amato et al., 2009; Zhao et al., 2006). Both total-mineral-mass and residual-mass approaches were used to calculate the reference dust mass. All the data we used were dust-dominated (dust fraction >50 wt%). More details about the data processing are described in Text S3 in Supporting Information S1. Insufficient dust-dominated data were available to evaluate the global equation for other types of anthropogenic dust including construction, combustion, and industrial dust (Pervez et al., 2018; Santacatalina et al., 2010; Z. Shen et al., 2016).

3. Results and Discussion

3.1. Characteristics of Regional MAL and CF Coefficients

The use of Si alone is explored first given its dominant abundance in dust. Figure S2 in Supporting Information S1 shows that the single Si coefficient M can vary by more than a factor of two within a region especially East Asia and Sahara where the standard deviation of M was 27% and 21% of the mean respectively. This high variability in the soil composition within the selected regions will result in undue errors in dust estimated using a single tracer, such as Si. Only the multi-component dust model is examined further.

We subsequently examine the use of regional MAL ratios. Table 2 shows dust data with negligible non-dust sources. The corresponding K/Fe ratios of desert dust in the southwestern US and eastern Asia are ~0.6 as used in the IMPROVE equation (Malm et al., 1994), but tend to be lower (~0.4) in other regions, providing evidence that the K/Fe ratio varies regionally. Figure 1 shows the variation of the MAL ratio in six different dust source regions and the MAL ratio for the average global continental crust using the data in Table 2. The median MAL ratio is significantly different ($P < 0.05$ for the Kruskal-Wallis test) across regions. Australia and the Sahel have low MAL ratios (<0.3) due to high chemical weathering (Kamber et al., 2005; Moreno et al., 2006, 2009; Reimann & de Caritat, 2012), while the MAL ratio in other regions is close to the crustal MAL ratio. Dust with relatively high MAL ratios (~0.8) in the Sahara (Linke et al., 2006; Moreno et al., 2006) and the Middle East (Hojati et al., 2012) is enriched in dolomite and palygorskite leading to their high Mg/Al ratios (>0.4). Figure S3 in Supporting Information S1 shows that the MSI ratio varies more widely than the MAL ratio both across and within regions, indicating that the sum of ($K_2O + MgO + Na_2O$) may associate better with Al than Si. This could be because Si has an additional major mineral source besides aluminosilicate, that is, quartz, which makes the MSI ratio sensitive to the variation of quartz content across and within regions (Nickovic et al., 2012) as well as the significant mineralogical fractionation effect on quartz (Ahmady-Birgani et al., 2015; Formenti et al., 2014; Jeong et al., 2014). Therefore, we used the MAL ratio instead of the MSI ratio to develop the global equation. No consistent difference of the MAL ratio among aerosol, soil, and sediment was observed. Thus, all the data were

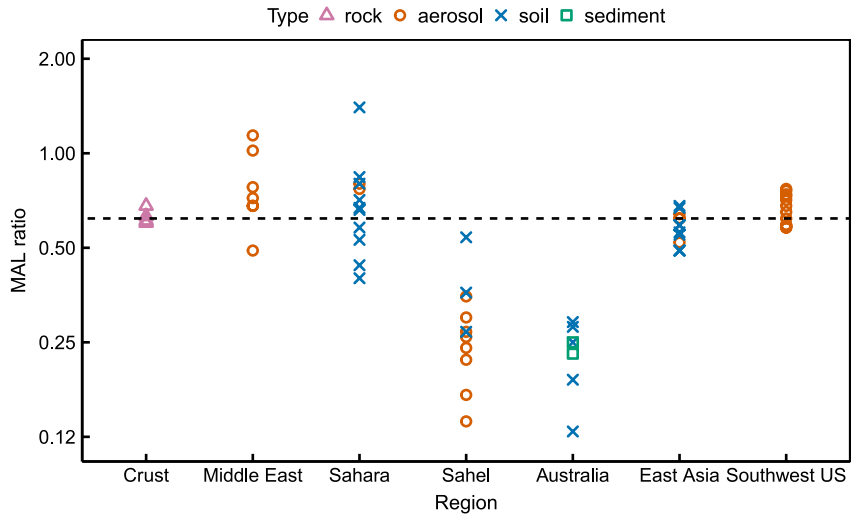

Figure 1. The mineral-to-aluminum (MAL) ratio of $(K_2O + MgO + Na_2O)/Al_2O_3$ in six dust source regions and the average global continental crust shown on a log scale. The dashed line indicates the median MAL ratio (0.62) in continental crust of four data sources. Each symbol represents a data record in Table 2.

used to develop regional MAL ratios. The particle size effect is discussed below. The median values in Table 2 were used to represent regional MAL ratios in six dust source regions and the crustal MAL ratio listed in Table 3.

The regional carbonate content and CF are thereafter investigated. Figure S4 in Supporting Information S1 demonstrates that $CaCO_3$ of topsoil is predominantly distributed in arid areas with variation in amounts across different deserts. The approximate content of $CaCO_3$ in topsoil for the six dust source regions is shown in Table 3, which generally agrees with available dust measurements in previous studies. Desert dust in the Middle East is commonly rich in carbonate due to abundant calcite and dolomite in local soils (Ahmady-Birgani et al., 2015; Awadh, 2012; Modaihsh, 1997). Saharan dust is considerably more carbonate-rich than Sahelian dust that is largely originated from the Chad Basin (Moreno et al., 2006; Scheuvens et al., 2013). The carbonate content of Australian dust is relatively low most likely linked to extensive and intense weathering of Australian soils (Moreno et al., 2009; Reimann & de Caritat, 2012). Asian dust in the Taklimakan Desert and Gobi area contains large amounts of carbonate (Cao, 2005; Wang et al., 2005). USGS reports somewhat higher calcite contents than the HWSD but they both show soils in the Southwest US are primarily carbonate-rich. Figure S5 in Supporting

Table 3
Region-Specific Mineral-to-Aluminum Ratio and Correction Factor for Natural Dust

Type	Region	Regional MAL	95% CI of MAL[a]	$CaCO_3$ (wt%)	CO_2 (wt%)	Regional CF
	Crust	0.62	(0.60, 0.68)		1	1.02
Source region	Middle East	0.72	(0.68, 1.00)	22	11	1.14
Source region	Sahara	0.69	(0.56, 0.80)	22	11	1.14
Source region	Sahel	0.27	(0.23, 0.35)	8	4	1.05
Source region	Australia	0.24	(0.19, 0.28)	8	4	1.05
Source region	East Asia	0.59	(0.54, 0.63)	18	9	1.11
Source region	Southwest US	0.66	(0.58, 0.71)	22	11	1.14
Within the US	East[b]	0.27				1.05
Within the US	West	0.66				1.14
Non-source region	South Europe and the Atlantic islands	0.48				1.10
Non-source region	Korea and Japan	0.59				1.11

[a]The 95% confidence interval of the median MAL ratio for six dust source regions (deserts) and the average global continental crust are calculated. [b]Eastern and western regions are defined based on the dividing line shown in Figure 3.

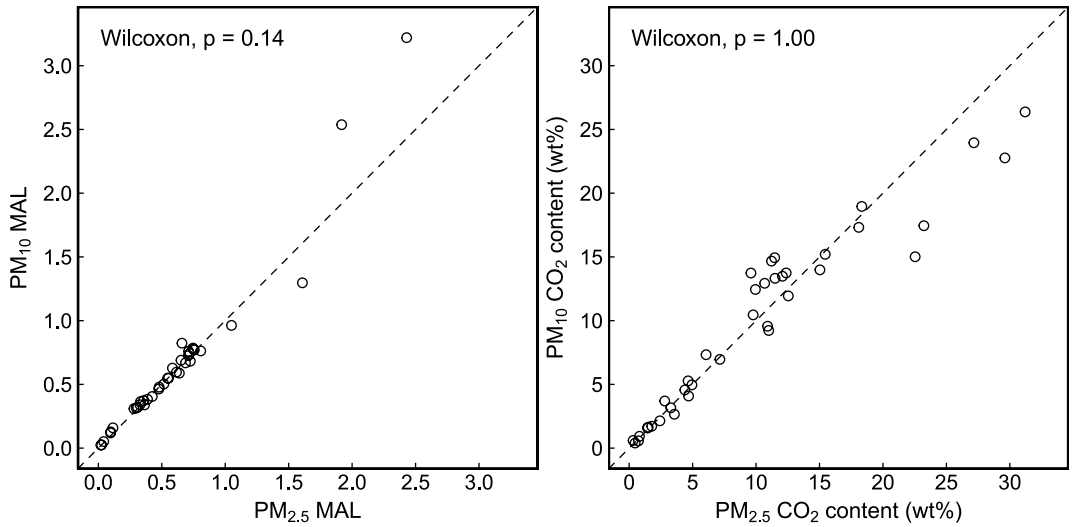

Figure 2. Particle size effect on the mineral-to-aluminum ratio and CO_2 content of dust using a data set of surface soil from arid regions (Engelbrecht et al., 2016). Inset *P*-values are the results of the paired-sample Wilcoxon test.

Information S1 shows that the mass ratio of total CO_2 to CO_2 in $CaCO_3$ is not significantly different across regions (Kruskal-Wallis test, $P > 0.05$). Hence, we applied the median ratio (1.11) of total CO_2 to CO_2 in $CaCO_3$ to account for other carbonates of dust in all the regions. Sensitivity tests using 25th percentile (1.06) or 75th percentile (1.20) for this mass ratio show that this variation does not significantly change the CF. The resulting dust CO_2 content and the calculated CF across six dust source regions and the average global continental crust are shown in Table 3. Although regional-scale variation in MAL and CF is included, microscale or synoptic-scale variation cannot be resolved without sufficient measured data.

We then examine the effects of particle size on the elemental ratios and CO_2 content. Figure S6 in Supporting Information S1 shows that using surface soil data from arid regions worldwide, the particle size of dust has a significant effect (paired-sample Wilcoxon test, $P < 0.05$) on Si/Al, Fe/Al, Ti/Al, and K/Al, but not on Ca/Al, Mg/Al, and Na/Al. As natural mechanical weathering can have various effects on minerals with different properties (Boose et al., 2016), the size effect is expected to differ among elemental ratios. However, Figure 2 indicates that the size effect is not significant for the MAL ratio (paired-sample Wilcoxon test, $P = 0.14$) and the CO_2 content (paired-sample Wilcoxon test, $P = 1.00$) which are used in the global equation. A size-dependent dust equation appears unnecessary based on the available data. Nevertheless, more available data sets of measured size-fractionated elemental composition and carbonate content of dust samples are needed to assess the size effect and possibly develop a size-dependent global dust equation.

The coefficients used within the US are further investigated. Figure 3 shows the distribution of the MAL ratio at IMPROVE sites. Most of the western sites have a similar MAL ratio with deserts in the Southwest, while the MAL ratio at eastern sites is close to that of Sahelian dust (~0.27). A previous study (Perry et al., 1997) found that African dust transported to the US has a characteristic Ca/Al ratio of <0.26, similar to that of Sahelian dust (median Ca/Al = 0.13 shown in Table 2). Thus, we applied the coefficients of Sahelian dust (MAL = 0.27, CF = 1.05) to eastern sites and those of the Southwest (MAL = 0.66, CF = 1.12) to western sites using the longitude (103.2°W) of the Big Bend national park (NP) site in Texas as an approximate dividing line based on the data pattern shown in Figure 3. Because we only use dust-dominated data to investigate the MAL pattern, using the Sahelian MAL may underestimate dust mass for months without the influence of African dust but the dust contribution to total $PM_{2.5}$ is small in those months.

Coefficients for desert dust transported to non-source regions are assumed to be the same as those used for source regions. Elemental ratios (e.g., Al/Ca, K/Fe) are used as dust source tracers in many studies and the elemental ratios used to calculate MAL (i.e., K/Al, Mg/Al, and Na/Al) can remain similar during long-range transport (e.g., Cao et al., 2008; Hand et al., 2017; Mori et al., 2003; VanCuren, 2002), so we used the MAL ratio of source regions for non-source regions. Previous studies show that $CaCO_3$ may be converted to $Ca(NO_3)_2$ or $CaSO_4$ by reacting with acidic species if the dust plume passes over highly polluted regions (Huang et al., 2010; Scheuvens

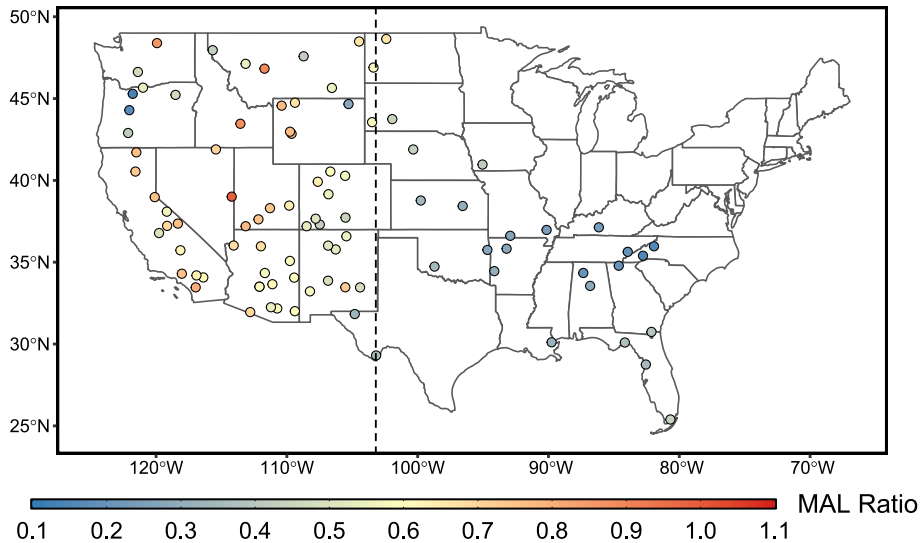

Figure 3. The mineral-to-aluminum ratio of $(K_2O + MgO + Na_2O)/Al_2O_3$ at Interagency Monitoring of Protected Visual Environments (IMPROVE) sites using daily-integrated dust-dominated (SOIL > 50% of reconstructed fine mass) $PM_{2.5}$ speciation data in 2011–2018 from the U.S. IMPROVE network. Only the sites with ≥5 data points were used to ensure representativeness. The number of selected IMPROVE sites is 95. The dashed line indicates the dividing line (103.2°W) through the Big Bend National Park site.

et al., 2013). Asian dust transported eastwards passing over urban areas of China can become aged (Heim et al., 2020), which may require a higher CF than that for Asian dust in the source region given the formation of secondary salts and adsorbed water due to increased hygroscopicity. The expanded expression of the global equation can be used in this case, but insufficient mineralogical information and hygroscopicity measurements are available to calculate the coefficients. Therefore, for Asian dust transported to Japan and Korea (K. H. Kim et al., 2003; Nishikawa et al., 1991), we still utilized the MAL ratio (0.59) and CF (1.11) of its source region. The loss of carbonate during long-range transport is not severe for African dust (Coz et al., 2009; Denjean et al., 2015; Scheuvens et al., 2013). African dust traveling to southern Europe (Alastuey et al., 2016; Escudero, 2005; Sánchez de la Campa et al., 2013; Stuut et al., 2009) and the Atlantic islands (Criado & Dorta, 2003; Engelbrecht et al., 2014; Formenti, 2003; Reid, 2003) can originate from both the Sahara and Sahel, so we employed the average MAL ratio (0.48) and average CF (1.10) of the two regions.

With limited data for different types of anthropogenic dust in various regions, we estimate the coefficients for anthropogenic dust more simplistically than for natural dust. The crustal MAL ratio (0.62) was applied to both paved road and unpaved road dust. Given that the road dust data are from areas (Texas, Illinois, northeastern Spain, and northern China) where local soils are enriched in carbonates or places affected by dust storms (Amato et al., 2009; Smith et al., 2019; Zhao et al., 2006), we used a high CF of 1.12 for both paved road and unpaved road dust. For agricultural soils, mobile elements (Na, K, and Mg) and carbonates can be leached by irrigation (Chow et al., 2003), so we applied a lower MAL ratio of 0.31 (half the crustal MAL) and the crustal CF (1.02).

3.2. Evaluation of the Global Dust Equation

Figure 4 shows the performance of the global equation and the IMPROVE equation for desert dust in six source regions and for the average global continental crust. The estimates by the global equation are consistent with the "total mineral mass" with a small NMB of −0.7%–0.2% and a small MFB of −0.7%–0.3% for all the source regions as well as the continental crust, while both the NMB and MFB of applying the IMPROVE equation are −6%–10%. Because the same CF was used in both the global equation and "total mineral mass," the comparison between the two estimates indicates the accuracy of applying the region-specific MAL ratio. Although the MAL ratio can vary by more than a factor of 4 within a region (Figure 1), the resulting bias in using a median MAL in each region is within ±1%. The underestimation of US desert dust by the IMPROVE equation is also observed in previous studies (Hand et al., 2019; Simon et al., 2010, 2011). Therefore, it is necessary to consider the variation in dust composition to improve the accuracy of estimating dust mass. Using an equation with region-specific

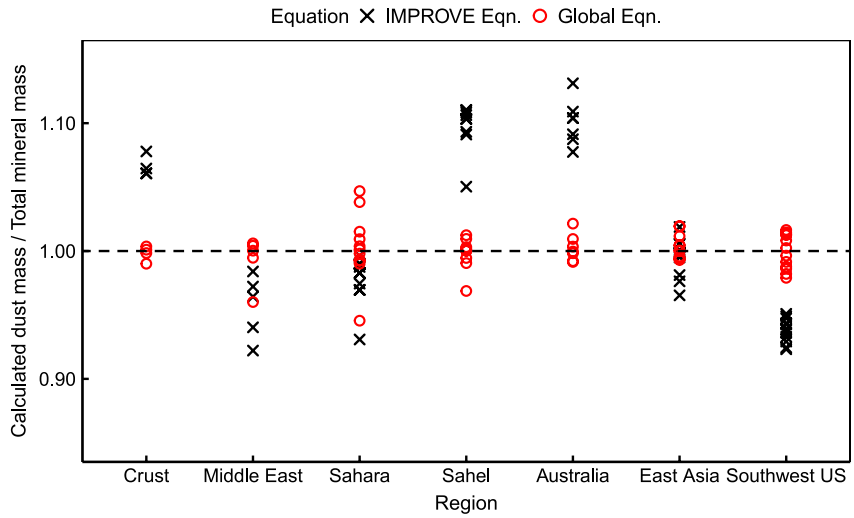

Figure 4. The ratio of the dust mass calculated by the global equation and the Interagency Monitoring of Protected Visual Environments (IMPROVE) equation to the "total mineral mass" for desert dust in source regions and for the average global continental crust.

coefficients (MAL and CF) is found to be an effective approach, which reduced the regional bias by about 6%–10% compared to the IMPROVE equation with universal coefficients. This reduction in bias matters to PM mass closure and model evaluation especially when dust mass is high during dust events. Although the global equation agrees well with the "total mineral mass," the total-mineral-mass approach cannot be used when Na, Mg, and K are significantly influenced by non-dust sources because they are directly added to the total dust mass. Thus, the advantage of the global equation is that it accounts for only the dust component of these elements by applying an average MAL ratio obtained from analyses of dust data with negligible non-dust sources.

The performance of the global equation for the IMPROVE network is shown in Figure 5. Both equations show a small bias compared to the "total mineral mass" (NMB and MFB within ±4%), which is within experimental uncertainties for the five elements (Al, Si, Ca, Fe, and Ti) measured in the IMPROVE network (Gorham et al., 2021; Hyslop & White, 2009). The global equation shows a slightly smaller NRMSE (8.5%) than the IMPROVE equation (10%). Applying the bootstrapping method, the mean estimates from the two equations have no statistically significant difference ($P = 0.30$). We also attempted to use the residual-mass approach for evaluation but were stymied by possible biases in gravimetric and speciated measurements as well as related assumptions. The relative humidity is not rigorously controlled in the weighing laboratory (Simon et al., 2011), especially after the laboratory was relocated in 2011, and RH generally increased after 2011 (Hand et al., 2019). Opposing biases from the residual-mass approach were observed before and after the IMPROVE weighing laboratory move in 2011, with no net bias as shown in Figure S7 in Supporting Information S1. Over the high dust mass range (>10 μg/m^3), the "residual mass" tended to be larger than estimates from the global equation after 2011, likely related to underestimated PBW, and tended to be smaller before 2011, possibly attributable to overestimated OM/OC ratio and the assumption of fully neutralized AS as discussed in Hand et al. (2019). The analytical changes in 2011 on dust could also contribute to the bias. Based on the IMPROVE advisory, the attenuation effect for light elements at high sample loadings was not corrected after the switch to the PANalytical XRF system and the implemented correction before 2011 could overcorrect the attenuation.

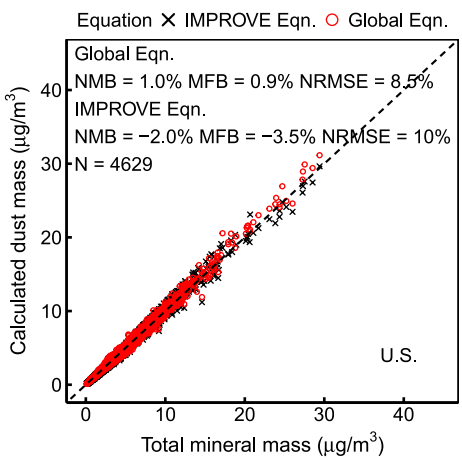

Figure 5. Comparison of the dust mass calculated by the global equation and the Interagency Monitoring of Protected Visual Environments (IMPROVE) equation with the "total mineral mass" using dust-dominated (SOIL > 50% reconstructed fine mass) $PM_{2.5}$ data in 2011–2018 from the U.S. IMPROVE network. Inset statistics are the normalized mean bias (NMB), mean fractional bias (MFB), and normalized root mean square error (NRMSE) of using the two equations for the entire data set. N is the number of speciation profiles.

Despite the overall systematic, yet unquantified, bias in the residual mass approach at IMPROVE sites, comparison across sites remains instructive because all sites are similarly affected by laboratory protocols. Figure 6

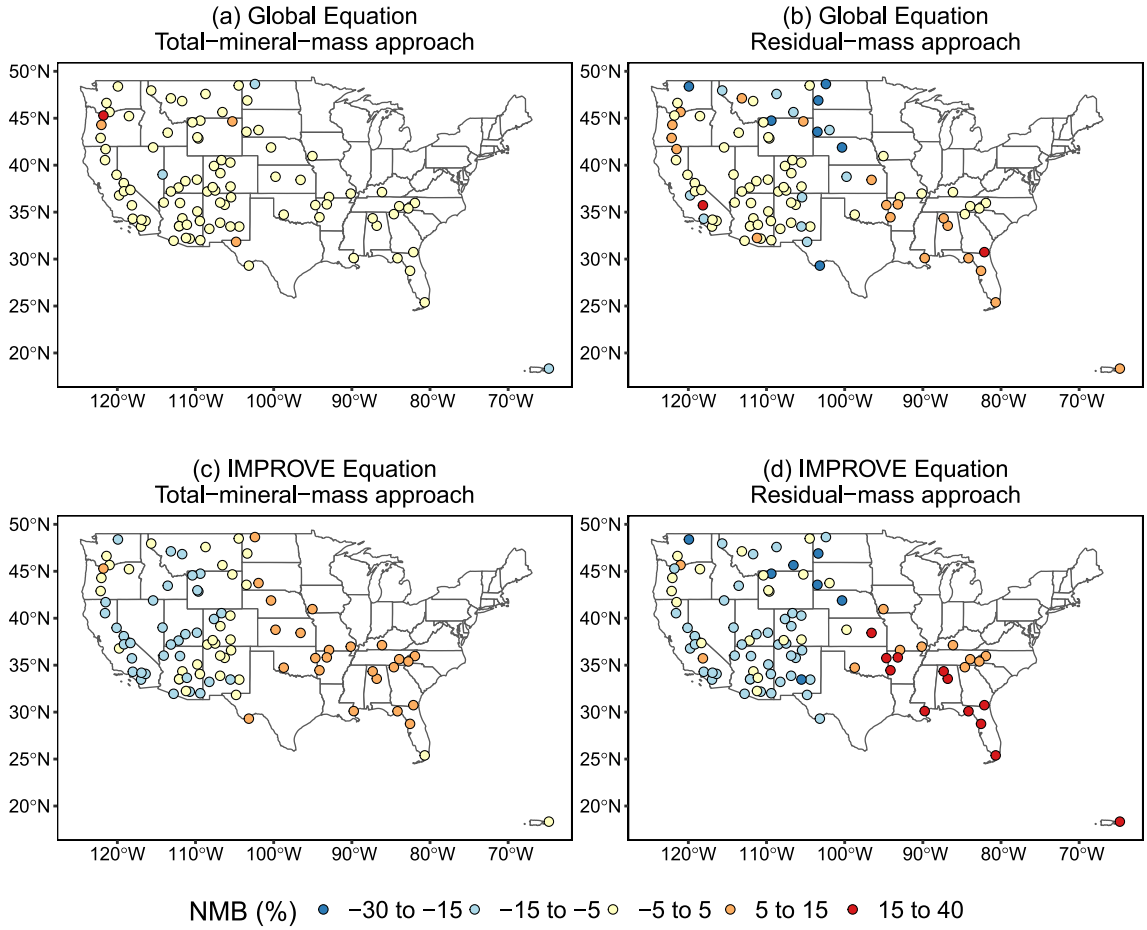

Figure 6. Normalized mean bias (NMB) for the dust mass calculated by (a and b) the global equation and (c and d) the Interagency Monitoring of Protected Visual Environments (IMPROVE) equation compared to (a and c) the "total mineral mass" and (b and d) the "residual mass" at IMPROVE sites using daily-integrated dust-dominated (SOIL > 50% of reconstructed fine mass) $PM_{2.5}$ speciation data in 2011–2018 from the U.S. IMPROVE network. Only the sites with ≥5 data points were used to ensure representativeness. The number of selected IMPROVE sites is 95.

presents the performance of the global equation at individual U.S. IMPROVE sites including the Virgin Islands NP site which is known to be impacted by African dust (Perry et al., 1997). Compared to the "total mineral mass," the global equation performs well at almost all sites (NMB within ±5%) and reduces the variable performance found for the IMPROVE equation. The residual-mass approach shows similar improvement after using the global equation, although overestimation or underestimation was observed at some sites possibly related to the heterogeneity of soil carbonate content on a small scale (Smith et al., 2019). Soils in the West Coast region of the US are carbonate-poor due to Mediterranean climates (Machette, 1985; Smith et al., 2019), which may explain the overestimation at some sites in that region. The underestimation at the Pasayten site (48.4°N, 119.9°W) in the Northwest may be attributable to the influence of transported Asian dust (Hand et al., 2012, 2017). For the Virgin Islands NP site, the global equation shows a much lower bias (NMB = 5.7%) than the IMPROVE equation (NMB = 15.9%). The overall improvement at IMPROVE sites is owing to the use of distinct MAL and CF for eastern and western sites in the global equation. Similar maps for MFB are shown in Figure S8 in Supporting Information S1.

Evaluation of the global equation for Europe is challenging due to the paucity of complete analyses of PM speciation and the strong effect of sea salt and biomass burning on the data (Manders et al., 2010; Sigsgaard et al., 2015), as well as the transport of dust from both the Sahara and Sahel with different dust mineralogy. We identified a campaign in Italy with sufficient characterization to contribute to the evaluation of the global equation. Figure 7 shows that both the global equation and the IMPROVE equation perform well for African dust transported to Italy using the total-mineral-mass and residual-mass approaches. The global equation shows

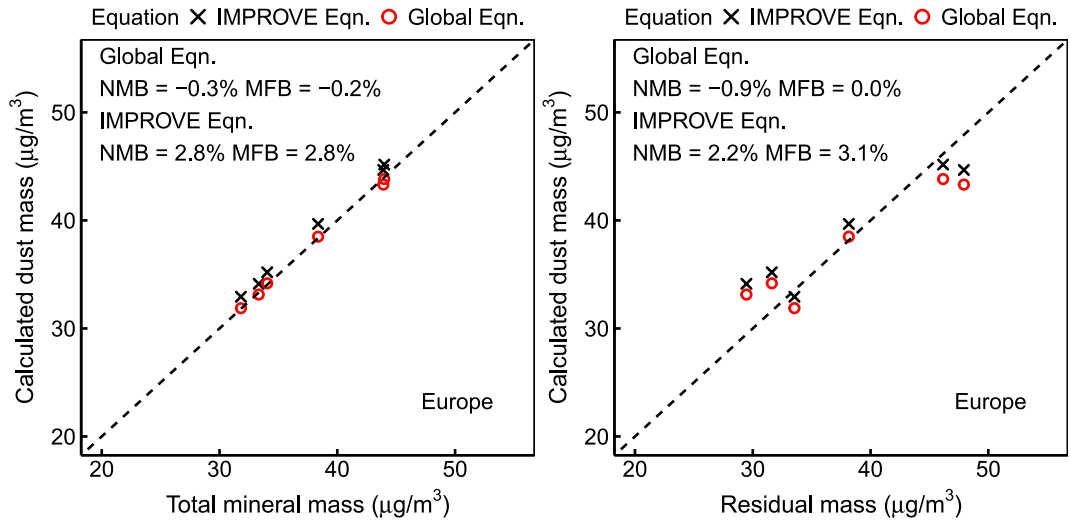

Figure 7. Comparison of dust mass calculated by the global equation and the Interagency Monitoring of Protected Visual Environments (IMPROVE) equation with the "total mineral mass" (left) and the "residual mass" (right) for dust-dominated PM_{10} data (SOIL > 50% of reconstructed fine mass) measured at Montelibretti, Italy during an African dust event (20–30 June 2006). Data with Na/Al > 0.45 or K/Al > 0.5 are excluded to reduce the influence of non-dust sources. Inset statistics are the normalized mean bias and mean fractional bias of using the two equations.

a somewhat lower NMB (−0.3% and −0.9% respectively) than the IMPROVE equation (2.8% and 2.1% respectively) for both approaches. The MFB of using the global equation (−0.2% and −0.0% respectively) is also somewhat lower than the IMPROVE equation (2.8% and 3.0% respectively) for both approaches. The performance of the global equation at EMEP sites during other African dust episodes is shown in Figure S9 in Supporting Information S1. The high correlation between the estimates by the global equation and "total mineral mass" indicates that the MAL ratio (0.48) in the global equation used for African dust transported to southern Europe is appropriate for data examined in Figure S9 in Supporting Information S1. The small difference between the estimates by the global equation and IMPROVE equation indicates that the fractions of missing compounds considered in both equations are close to each other in this case. However, for desert dust significantly depleted or enriched in mobile elements and carbonate, the difference will be larger as shown in Figure 4.

We evaluated the global equation for transported African dust over the Atlantic islands as well as transported Asian dust over Japan and Korea shown in Figure S10 in Supporting Information S1. For African dust, the global equation shows a slightly lower bias (NMB = 1.4%, MFB = 1.6%) than the IMPROVE equation (NMB = 2.0%, MFB = 1.7%). As for Asian dust, the global equation (NMB = −1.2%, MFB = −1.2%) performs similarly to the IMPROVE equation (NMB = −1.0%, MFB = −1.0%). The good performance of the global equation for desert dust over both source and non-source regions confirms that long-range transport does not substantially alter the MAL ratio of desert dust. However, the dust mass could be underestimated because the potential secondary salts and adsorbed water due to chemical aging are not included. Sufficient mineralogical information and hygroscopicity measurements are needed to better estimate transported dust that likely undergoes significant chemical aging.

Figure 8 shows the performance of the global equation and the IMPROVE equation for several major types of anthropogenic fugitive dust including paved road, unpaved road, and agricultural soil dust. Using the total-mineral-mass approach, the NMB for the global equation is similar to the IMPROVE equation for paved (3.3% vs. 2.4%) and unpaved (−0.05% vs. 1.1%) roads, while the bias for the global equation is much lower than the IMPROVE equation for agricultural soils (1.9% vs. 15%). Similar results were found using the residual mass as the reference, although more noise was observed which is attributable to greater uncertainties in calculating the residual mass. The results suggest that the previously recognized overestimate by the IMPROVE equation of agricultural soil (Simon et al., 2010, 2011) can be remedied by accounting for the depletion of mobile elements and carbonates by irrigation. Because the evaluation is based on data with limited regional coverage, more measured data of anthropogenic dust in different regions are needed to further examine the performance of the global equation. It is difficult to derive general coefficients (MAL and CF) for other types of anthropogenic dust because

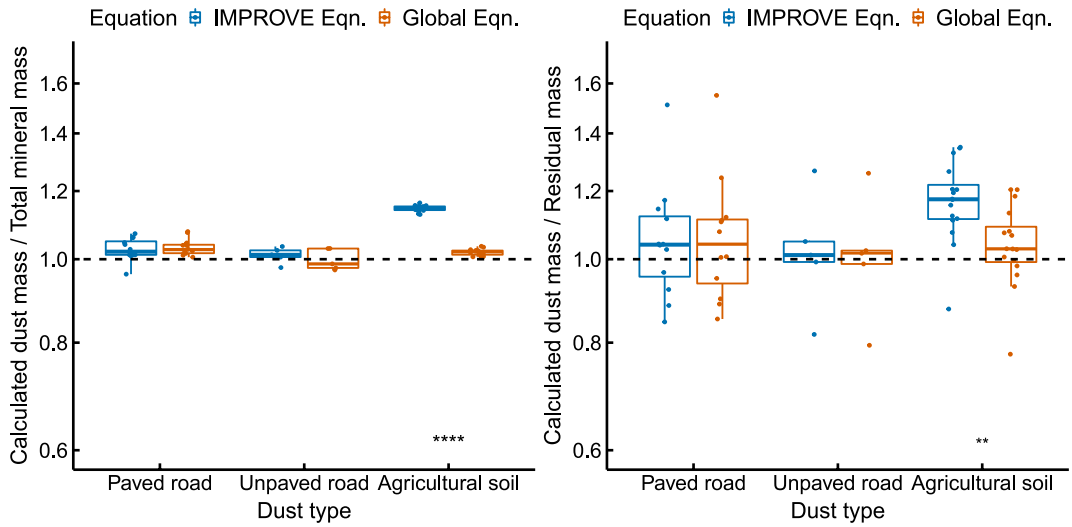

Figure 8. The ratio of the dust mass calculated by the global equation and the Interagency Monitoring of Protected Visual Environments (IMPROVE) equation to the "total mineral mass" (left) and the "residual mass" (right) for paved road, unpaved road, and agricultural soil dust using $PM_{2.5}$ and PM_{10} data from the U.S. Environmental Protection Agency's SPECIATE database and collected literature data (Amato et al., 2009; Zhao et al., 2006). Ratios are presented on a log scale. Data points are jittered to avoid overlap. The number of asterisks indicates the significance level (**$P < 0.01$, ****$P < 0.0001$) of the difference between two groups using the paired-sample Wilcoxon test.

their chemical composition can vary widely depending on the source and the area. However, an accurate dust equation is still important to estimate the concentration of different types of anthropogenic dust if the missing compounds are not measured or some crustal elements have significant non-dust sources.

4. Conclusions

This study develops a global-scale mineral dust equation used to estimate dust mass by building upon the IMPROVE equation that was designed for the U.S. The IMPROVE equation is widely used to calculate dust mass but prior work finds general underestimates in dust mass across the IMPROVE network, and had not been evaluated globally. Developing a global dust equation needs to address several issues especially the variation of dust composition across different regions. Three important mineral compounds, K_2O, MgO, and Na_2O, are usually either missing from previous dust equations or directly included without excluding biomass burning or sea salt sources. Our global dust equation incorporates the three compounds using Al as a surrogate by defining the MAL ratio as $(K_2O + MgO + Na_2O)/Al_2O_3$ that is specific to the dust components of K, Mg, and Na. Analyses of dust data from major dust source regions of the world with negligible non-dust sources indicate that the MAL ratio is significantly different across regions with Australian and Sahelian dust exhibiting much lower MAL ratios than dust in other regions. A CF is used to account for other missing compounds, mainly CO_2 which is an important mineral compound but is commonly not measured and not included in previous dust equations. The amount of CO_2 in dust inferred from $CaCO_3$ content in topsoil and mineralogical data also varies substantially across regions. We provide flexible options for expanding the global equation to include adsorbed water and salt minerals in special types of dust such as saline dust, volcanic dust, and aged dust.

Applying the global dust equation with the region-specific coefficients (MAL and CF) to major dust source regions and using the IMPROVE equation as a benchmark demonstrates that the global equation provides evident improvement for estimating the dust mass. Compared to the reference dust mass, the resulting NMB and MFB of the estimates from the global equation are within ±1%, while those from the IMPROVE equation are −6%–10%. The global equation also performs well (NMB and MFB within ±2%) for desert dust transported to non-source regions using coefficients that depend on their source regions. For major types of anthropogenic dust (paved road, unpaved road, and agricultural soil), the global equation generally performs well (NMB within ±5%) by applying the crustal MAL ratio and a high CF for road dust as well as a low MAL and CF for agricultural soil dust. Applying different coefficients to eastern and western IMPROVE sites, the global equation estimates the dust mass well (NMB within ±5%) at most sites.

Further improvement of the global equation would benefit from more complete and accurate measurements of mineral elements and CO_2 content in dust. More accurate estimation of OM, sea salt, and PBW can decrease the uncertainties in calculating the reference dust mass using the residual-mass approach. Assigning the coefficients on a finer spatial scale could further reduce the bias but would require much more data. Further examining the link of the MAL ratio and carbonate content between soil and aerosol is beyond the scope of our work but worthy of further study. Characteristics of different types of anthropogenic dust over various regions deserve further investigation. Despite the limitations, the global equation with region-specific coefficients has an absolute advantage over the IMPROVE equation with universal coefficients because it considers the variation in dust composition across different regions which is important for accurate estimation of dust mass on a global scale.

To our knowledge, this is the first study to develop and evaluate a region-specific global dust equation, which is challenging given the limitation of insufficient complete measurements of dust composition on a global scale and the lack of an absolute benchmark for reference dust mass. The use of regional coefficients for MAL and CF yields a promising method for estimating the dust mass not only outside the US but also within the US. This global equation can help future studies assess the measured dust contribution to aerosols more accurately when performing PM mass reconstruction and better understand the dust impacts on the environment and human health. More accurate representation of ground-based dust measurements can also benefit the development of atmospheric models and satellite remote sensing algorithms.

Data Availability Statement

The elemental composition data from the U.S. Interagency Monitoring of Protected Visual Environments network is available at http://vista.cira.colostate.edu/Improve/improve-data/. The elemental composition data from the SPARTAN network can be downloaded at https://www.spartan-network.org/data. The elemental composition data from the EMEP sites can be accessed at http://ebas-data.nilu.no/default.aspx. The U.S. EPA's SPECIATE 5.0 database is available via https://www.epa.gov/air-emissions-modeling/speciate-2. The Harmonized World Soil Database can be found at https://webarchive.iiasa.ac.at/Research/LUC/External-World-soil-database/HTML/index.html?sb=1. All the collected data from literature with detailed data selection and processing are compiled into a data set available at https://data.mendeley.com/datasets/55vd6p28gk/1 (Liu, 2022).

Acknowledgments
This work was funded by the National Science Foundation (Grant 2020673), the Clean Air Fund, and internal funds at Washington University in St. Louis. Randall V. Martin and Jay R. Turner equally supervised and equally funded this research. Interagency Monitoring of Protected Visual Environments is a collaborative association of state, tribal, and federal agencies, and international partners. US Environmental Protection Agency is the primary funding source, with contracting and research support from the National Park Service. The Air Quality Group at the University of California, Davis is the central analytical laboratory, with ion analysis provided by Research Triangle Institute, and carbon analysis provided by Desert Research Institute.

References

Abed, A. M., Al Kuisi, M., & Khair, H. A. (2009). Characterization of the Khamaseen (spring) dust in Jordan. *Atmospheric Environment*, *43*(18), 2868–2876. https://doi.org/10.1016/j.atmosenv.2009.03.015

Ahmady-Birgani, H., Mirnejad, H., Feiznia, S., & McQueen, K. G. (2015). Mineralogy and geochemistry of atmospheric particulates in western Iran. *Atmospheric Environment*, *119*, 262–272. https://doi.org/10.1016/j.atmosenv.2015.08.021

Alastuey, A., Querol, X., Aas, W., Lucarelli, F., Pérez, N., Moreno, T., et al. (2016). Geochemistry of PM10 over Europe during the EMEP intensive measurement periods in summer 2012 and winter 2013. *Atmospheric Chemistry and Physics*, *16*(10), 6107–6129. https://doi.org/10.5194/acp-16-6107-2016

Alfaro, S. C. (2003). Chemical and optical characterization of aerosols measured in spring 2002 at the ACE-Asia supersite, Zhenbeitai, China. *Journal of Geophysical Research*, *108*(D23), 8641. https://doi.org/10.1029/2002JD003214

Amato, F., Pandolfi, M., Viana, M., Querol, X., Alastuey, A., & Moreno, T. (2009). Spatial and chemical patterns of PM10 in road dust deposited in urban environment. *Atmospheric Environment*, *43*(9), 1650–1659. https://doi.org/10.1016/j.atmosenv.2008.12.009

Andrews, E., Saxena, P., Musarra, S., Hildemann, L. M., Koutrakis, P., McMurry, P. H., et al. (2000). Concentration and composition of atmospheric aerosols from the 1995 SEAVS experiment and a review of the closure between chemical and gravimetric measurements. *Journal of the Air & Waste Management Association*, *50*(5), 648–664. https://doi.org/10.1080/10473289.2000.10464116

Appel, K. W., Pouliot, G. A., Simon, H., Sarwar, G., Pye, H. O. T., Napelenok, S. L., et al. (2013). Evaluation of dust and trace metal estimates from the Community Multiscale Air Quality (CMAQ) model version 5.0. *Geoscientific Model Development*, *6*(4), 883–899. https://doi.org/10.5194/gmd-6-883-2013

Arimoto, R. (2004). Chemical composition of atmospheric aerosols from Zhenbeitai, China, and Gosan, South Korea, during ACE-Asia. *Journal of Geophysical Research*, *109*(D19), D19S04. https://doi.org/10.1029/2003JD004323

Ashley, W. S., Strader, S., Dziubla, D. C., & Haberlie, A. (2015). Driving blind: Weather-related vision hazards and fatal motor vehicle crashes. *Bulletin of the American Meteorological Society*, *96*(5), 755–778. https://doi.org/10.1175/BAMS-D-14-00026.1

Awadh, S. M. (2012). Geochemistry and mineralogical composition of the airborne particles of sand dunes and dust storms settled in Iraq and their environmental impacts. *Environmental Earth Sciences*, *66*(8), 2247–2256. https://doi.org/10.1007/s12665-011-1445-6

Boose, Y., Welti, A., Atkinson, J., Ramelli, F., Danielczok, A., Bingemer, H. G., et al. (2016). Heterogeneous ice nucleation on dust particles sourced from nine deserts worldwide – Part 1: Immersion freezing. *Atmospheric Chemistry and Physics*, *16*(23), 15075–15095. https://doi.org/10.5194/acp-16-15075-2016

Cao, J. J. (2005). Characterization of airborne carbonate over a site near Asian dust source regions during spring 2002 and its climatic and environmental significance. *Journal of Geophysical Research*, *110*(D3), D03203. https://doi.org/10.1029/2004JD005244

Cao, J. J., Chow, J. C., Watson, J. G., Wu, F., Han, Y. M., Jin, Z. D., et al. (2008). Size-differentiated source profiles for fugitive dust in the Chinese Loess Plateau. *Atmospheric Environment*, *42*(10), 2261–2275. https://doi.org/10.1016/j.atmosenv.2007.12.041

Chen, H., Laskin, A., Baltrusaitis, J., Gorski, C. A., Scherer, M. M., & Grassian, V. H. (2012). Coal fly ash as a source of iron in atmospheric dust. *Environmental Science & Technology*, *46*(4), 2112–2120. https://doi.org/10.1021/es204102f

Choi, J. C., Lee, M., Chun, Y., Kim, J., & Oh, S. (2001). Chemical composition and source signature of spring aerosol in Seoul, Korea. *Journal of Geophysical Research*, *106*(D16), 18067–18074. https://doi.org/10.1029/2001JD900090

Chow, J. C., Lowenthal, D. H., Chen, L.-W. A., Wang, X., & Watson, J. G. (2015). Mass reconstruction methods for PM2.5: A review. *Air Quality, Atmosphere & Health*, *8*(3), 243–263. https://doi.org/10.1007/s11869-015-0338-3

Chow, J. C., Watson, J. G., Ashbaugh, L. L., & Magliano, K. L. (2003). Similarities and differences in PM10 chemical source profiles for geological dust from the San Joaquin Valley, California. *Atmospheric Environment*, *37*(9–10), 1317–1340. https://doi.org/10.1016/S1352-2310(02)01021-X

Chow, J. C., Watson, J. G., Fujita, E. M., Lu, Z., Lawson, D. R., & Ashbaugh, L. L. (1994). Temporal and spatial variations of $PM_{2.5}$ and PM_{10} aerosol in the Southern California air quality study. *Atmospheric Environment*, *28*(12), 2061–2080. https://doi.org/10.1016/1352-2310(94)90474-X

Claquin, T., Schulz, M., & Balkanski, Y. J. (1999). Modeling the mineralogy of atmospheric dust sources. *Journal of Geophysical Research*, *104*(D18), 22243–22256. https://doi.org/10.1029/1999JD900416

Contini, D., Genga, A., Cesari, D., Siciliano, M., Donateo, A., Bove, M. C., & Guascito, M. R. (2010). Characterisation and source apportionment of PM10 in an urban background site in Lecce. *Atmospheric Research*, *95*(1), 40–54. https://doi.org/10.1016/j.atmosres.2009.07.010

Coz, E., Gómez-Moreno, F. J., Pujadas, M., Casuccio, G. S., Lersch, T. L., & Artíñano, B. (2009). Individual particle characteristics of North African dust under different long-range transport scenarios. *Atmospheric Environment*, *43*(11), 1850–1863. https://doi.org/10.1016/j.atmosenv.2008.12.045

Criado, C., & Dorta, P. (2003). An unusual "blood rain" over the Canary Islands (Spain). The storm of January 1999. *Journal of Arid Environments*, *55*(4), 765–783. https://doi.org/10.1016/S0140-1963(02)00320-8

Deboudt, K., Flament, P., Choël, M., Gloter, A., Sobanska, S., & Colliex, C. (2010). Mixing state of aerosols and direct observation of carbonaceous and marine coatings on African dust by individual particle analysis. *Journal of Geophysical Research*, *115*(D24), D24207. https://doi.org/10.1029/2010jd013921

Denjean, C., Caquineau, S., Desboeufs, K., Laurent, B., Maille, M., Quiñones Rosado, M., et al. (2015). Long-range transport across the Atlantic in summertime does not enhance the hygroscopicity of African mineral dust. *Geophysical Research Letters*, *42*(18), 7835–7843. https://doi.org/10.1002/2015GL065693

Diner, D. J., Boland, S. W., Brauer, M., Bruegge, C., Burke, K. A., Chipman, R., et al. (2018). Advances in multiangle satellite remote sensing of speciated airborne particulate matter and association with adverse health effects: From MISR to MAIA. *Journal of Applied Remote Sensing*, *12*(4), 042603. https://doi.org/10.1117/1.JRS.12.042603

Eldred, B. (2003). Evaluation of the equation for soil composite: Internal memo to IMPROVE staff.

Engelbrecht, J. P., Menéndez, I., & Derbyshire, E. (2014). Sources of PM2.5 impacting on gran Canaria, Spain. *Catena*, *117*, 119–132. https://doi.org/10.1016/j.catena.2013.06.017

Engelbrecht, J. P., Moosmüller, H., Pincock, S., Jayanty, R. K. M., Lersch, T., & Casuccio, G. (2016). Technical note: Mineralogical, chemical, morphological, and optical interrelationships of mineral dust re-suspensions. *Atmospheric Chemistry and Physics*, *16*(17), 10809–10830. https://doi.org/10.5194/acp-16-10809-2016

Escudero, M. (2005). Wet and dry African dust episodes over eastern Spain. *Journal of Geophysical Research*, *110*(D18), D18S08. https://doi.org/10.1029/2004JD004731

FAO, I., & ISRIC, I. (2012). JRC: Harmonized world soil database (version 1.2) [Dataset]. FAO, Rome, Italy and IIASA. https://webarchive.iiasa.ac.at/Research/LUC/External-World-soil-database/HTML/HWSD_Data.html?sb=4

Formenti, P. (2003). Chemical composition of mineral dust aerosol during the Saharan Dust Experiment (SHADE) airborne campaign in the Cape Verde region, September 2000. *Journal of Geophysical Research*, *108*(D18), 8576. https://doi.org/10.1029/2002JD002648

Formenti, P., Caquineau, S., Desboeufs, K., Klaver, A., Chevaillier, S., Journet, E., & Rajot, J. L. (2014). Mapping the physico-chemical properties of mineral dust in western Africa: Mineralogical composition. *Atmospheric Chemistry and Physics*, *14*(19), 10663–10686. https://doi.org/10.5194/acp-14-10663-2014

Formenti, P., Rajot, J. L., Desboeufs, K., Caquineau, S., Chevaillier, S., Nava, S., et al. (2008). Regional variability of the composition of mineral dust from western Africa: Results from the AMMA SOP0/DABEX and DODO field campaigns. *Journal of Geophysical Research*, *113*(D23), D00C13. https://doi.org/10.1029/2008JD009903

Ganor, E., Foner, H. A., Brenner, S., Neeman, E., & Lavi, N. (1991). The chemical composition of aerosols settling in Israel following dust storms. *Atmospheric Environment, Part A: General Topics*, *25*(12), 2665–2670. https://doi.org/10.1016/0960-1686(91)90196-E

Gao, J., Wang, K., Wang, Y., Liu, S., Zhu, C., Hao, J., et al. (2018). Temporal-spatial characteristics and source apportionment of PM2.5 as well as its associated chemical species in the Beijing-Tianjin-Hebei region of China. *Environmental Pollution*, *233*, 714–724. https://doi.org/10.1016/j.envpol.2017.10.123

Gaston, C. J. (2020). Re-Examining dust chemical aging and its impacts on Earth's climate. *Accounts of Chemical Research*, *53*(5), 1005–1013. https://doi.org/10.1021/acs.accounts.0c00102

Gaston, C. J., Pratt, K. A., Suski, K. J., May, N. W., Gill, T. E., & Prather, K. A. (2017). Laboratory studies of the cloud droplet activation properties and corresponding chemistry of saline playa dust. *Environmental Science & Technology*, *51*(3), 1348–1356. https://doi.org/10.1021/acs.est.6b04487

Gislason, S. R., Hassenkam, T., Nedel, S., Bovet, N., Eiriksdottir, E. S., Alfredsson, H. A., et al. (2011). Characterization of Eyjafjallajökull volcanic ash particles and a protocol for rapid risk assessment. *Proceedings of the National Academy of Sciences of the United States of America*, *108*(18), 7307–7312. https://doi.org/10.1073/pnas.1015053108

Gomes, L., Bergametti, G., Coudé-Gaussen, G., & Rognon, P. (1990). Submicron desert dust: A sandblasting process. *Journal of Geophysical Research*, *95*(D9), 13927. https://doi.org/10.1029/JD095iD09p13927

Gorham, K. A., Raffuse, S. M., Hyslop, N. P., & White, W. H. (2021). Comparison of recent speciated PM2.5 data from collocated CSN and IMPROVE measurements. *Atmospheric Environment*, *244*, 117977. https://doi.org/10.1016/j.atmosenv.2020.117977

Goudie, A. S. (2014). Desert dust and human health disorders. *Environment International*, *63*, 101–113. https://doi.org/10.1016/j.envint.2013.10.011

Hand, J. L., Gill, T. E., & Schichtel, B. A. (2017). Spatial and seasonal variability in fine mineral dust and coarse aerosol mass at remote sites across the United States: Fine mineral dust and coarse mass. *Journal of Geophysical Research: Atmospheres*, *122*(5), 3080–3097. https://doi.org/10.1002/2016JD026290

Hand, J. L., Prenni, A. J., Copeland, S., Schichtel, B. A., & Malm, W. C. (2020). Thirty years of the clean air act amendments: Impacts on haze in remote regions of the United States (1990–2018). *Atmospheric Environment*, *243*, 117865. https://doi.org/10.1016/j.atmosenv.2020.117865

Hand, J. L., Prenni, A. J., Schichtel, B. A., Malm, W. C., & Chow, J. C. (2019). Trends in remote PM2.5 residual mass across the United States: Implications for aerosol mass reconstruction in the IMPROVE network. *Atmospheric Environment*, *203*, 141–152. https://doi.org/10.1016/j.atmosenv.2019.01.049

Hand, J. L., Schichtel, B. A., Malm, W. C., Copeland, S., Molenar, J. V., Frank, N., & Pitchford, M. (2014). Widespread reductions in haze across the United States from the early 1990s through 2011. *Atmospheric Environment*, *94*, 671–679. https://doi.org/10.1016/j.atmosenv.2014.05.062

Hand, J. L., Schichtel, B. A., Pitchford, M., Malm, W. C., & Frank, N. H. (2012). Seasonal composition of remote and urban fine particulate matter in the United States: Composition of remote and urban aerosols. *Journal of Geophysical Research*, *117*(D5), D05209. https://doi.org/10.1029/2011JD017122

Heim, E. W., Dibb, J., Scheuer, E., Jost, P. C., Nault, B. A., Jimenez, J. L., et al. (2020). Asian dust observed during KORUS-AQ facilitates the uptake and incorporation of soluble pollutants during transport to South Korea. *Atmospheric Environment*, *224*, 117305. https://doi.org/10.1016/j.atmosenv.2020.117305

Herich, H., Tritscher, T., Wiacek, A., Gysel, M., Weingartner, E., Lohmann, U., et al. (2009). Water uptake of clay and desert dust aerosol particles at sub- and supersaturated water vapor conditions. *Physical Chemistry Chemical Physics*, *11*(36), 7804. https://doi.org/10.1039/b901585j

Ho, K. F., Lee, S. C., Chow, J. C., & Watson, J. G. (2003). Characterization of PM10 and PM2.5 source profiles for fugitive dust in Hong Kong. *Atmospheric Environment*, *37*(8), 1023–1032. https://doi.org/10.1016/S1352-2310(02)01028-2

Hojati, S., Khademi, H., Faz Cano, A., & Landi, A. (2012). Characteristics of dust deposited along a transect between central Iran and the Zagros Mountains. *Catena*, *88*(1), 27–36. https://doi.org/10.1016/j.catena.2011.09.002

Huang, K., Zhuang, G., Li, J., Wang, Q., Sun, Y., Lin, Y., & Fu, J. S. (2010). Mixing of Asian dust with pollution aerosol and the transformation of aerosol components during the dust storm over China in spring 2007. *Journal of Geophysical Research*, *115*, D00K13. https://doi.org/10.1029/2009JD013145

Hueglin, C., Gehrig, R., Baltensperger, U., Gysel, M., Monn, C., & Vonmont, H. (2005). Chemical characterisation of $PM_{2.5}$, PM_{10} and coarse particles at urban, near-city and rural sites in Switzerland. *Atmospheric Environment*, *39*(4), 637–651. https://doi.org/10.1016/j.atmosenv.2004.10.027

Hyslop, N. P., Trzepla, K., & White, W. H. (2015). Assessing the suitability of historical $PM_{2.5}$ element measurements for trend analysis. *Environmental Science & Technology*, *49*(15), 9247–9255. https://doi.org/10.1021/acs.est.5b01572

Hyslop, N. P., & White, W. H. (2009). Estimating precision using duplicate measurements. *Journal of the Air & Waste Management Association*, *59*(9), 1032–1039. https://doi.org/10.3155/1047-3289.59.9.1032

Ibrahim, S., Romanias, M. N., Alleman, L. Y., Zeineddine, M. N., Angeli, G. K., Trikalitis, P. N., & Thevenet, F. (2018). Water interaction with mineral dust aerosol: Particle size and hygroscopic properties of dust. *ACS Earth and Space Chemistry*, *2*(4), 376–386. https://doi.org/10.1021/acsearthspacechem.7b00152

Jeong, G. Y., Kim, J. Y., Seo, J., Kim, G. M., Jin, H. C., & Chun, Y. (2014). Long-range transport of giant particles in Asian dust identified by physical, mineralogical, and meteorological analysis. *Atmospheric Chemistry and Physics*, *14*(1), 505–521. https://doi.org/10.5194/acp-14-505-2014

Jickells, T. D., An, Z. S., Andersen, K. K., Baker, A. R., Bergametti, G., Brooks, N., et al. (2005). Global iron connections between desert dust, ocean biogeochemistry, and climate. *Science*, *308*(5718), 67–71. https://doi.org/10.1126/science.1105959

Journet, E., Balkanski, Y., & Harrison, S. P. (2014). A new data set of soil mineralogy for dust-cycle modeling. *Atmospheric Chemistry and Physics*, *14*(8), 3801–3816. https://doi.org/10.5194/acp-14-3801-2014

Kamber, B. S., Greig, A., & Collerson, K. D. (2005). A new estimate for the composition of weathered young upper continental crust from alluvial sediments, Queensland, Australia. *Geochimica et Cosmochimica Acta*, *69*(4), 1041–1058. https://doi.org/10.1016/j.gca.2004.08.020

Kandler, K., Benker, N., Bundke, U., Cuevas, E., Ebert, M., Knippertz, P., et al. (2007). Chemical composition and complex refractive index of Saharan Mineral Dust at Izaña, Tenerife (Spain) derived by electron microscopy. *Atmospheric Environment*, *41*(37), 8058–8074. https://doi.org/10.1016/j.atmosenv.2007.06.047

Kavouras, I. G., Etyemezian, V., DuBois, D. W., Xu, J., & Pitchford, M. (2009). Source reconciliation of atmospheric dust causing visibility impairment in Class I areas of the western United States. *Journal of Geophysical Research*, *114*(D2), D02308. https://doi.org/10.1029/2008JD009923

Khiri, F., Ezaidi, A., & Kabbachi, K. (2004). Dust deposits in Souss–Massa basin, south-west of Morocco: Granulometrical, mineralogical and geochemical characterisation. *Journal of African Earth Sciences*, *39*(3–5), 459–464. https://doi.org/10.1016/j.jafrearsci.2004.07.019

Kim, K. H., Choi, G. H., Kang, C. H., Lee, J. H., Kim, J. Y., Youn, Y. H., & Lee, S. R. (2003). The chemical composition of fine and coarse particles in relation with the Asian Dust events. *Atmospheric Environment*, *37*(6), 753–765. https://doi.org/10.1016/S1352-2310(02)00954-8

Kim, K. W., Kim, Y. J., & Oh, S. J. (2001). Visibility impairment during Yellow Sand periods in the urban atmosphere of Kwangju, Korea. *Atmospheric Environment*, *35*(30), 5157–5167. https://doi.org/10.1016/S1352-2310(01)00330-2

Kleindienst, T. E., Lewandowski, M., Offenberg, J. H., Edney, E. O., Jaoui, M., Zheng, M., et al. (2010). Contribution of primary and secondary sources to organic aerosol and $PM_{2.5}$ at SEARCH network sites. *Journal of the Air & Waste Management Association*, *60*(11), 1388–1399. https://doi.org/10.3155/1047-3289.60.11.1388

Koehler, K. A., Kreidenweis, S. M., DeMott, P. J., Petters, M. D., Prenni, A. J., & Carrico, C. M. (2009). Hygroscopicity and cloud droplet activation of Mineral Dust aerosol. *Geophysical Research Letters*, *36*(8), L08805. https://doi.org/10.1029/2009GL037348

Koehler, K. A., Kreidenweis, S. M., DeMott, P. J., Prenni, A. J., & Petters, M. D. (2007). Potential impact of Owens (dry) Lake dust on warm and cold cloud formation. *Journal of Geophysical Research*, *112*(D12), D12210. https://doi.org/10.1029/2007JD008413

Kok, J. F., Adebiyi, A. A., Albani, S., Balkanski, Y., Checa-Garcia, R., Chin, M., et al. (2021). Improved representation of the global dust cycle using observational constraints on dust properties and abundance. *Atmospheric Chemistry and Physics*, *21*(10), 8127–8167. https://doi.org/10.5194/acp-21-8127-2021

Koren, I., Kaufman, Y. J., Washington, R., Todd, M. C., Rudich, Y., Martins, J. V., & Rosenfeld, D. (2006). The Bodélé depression: A single spot in the Sahara that provides most of the mineral dust to the Amazon forest. *Environmental Research Letters*, *1*(1), 014005. https://doi.org/10.1088/1748-9326/1/1/014005

Kreidenweis, S. M., Petters, M. D., & DeMott, P. J. (2008). Single-parameter estimates of aerosol water content. *Environmental Research Letters*, *3*(3), 035002. https://doi.org/10.1088/1748-9326/3/3/035002

Latimer, R. N. C., & Martin, R. V. (2019). Interpretation of measured aerosol mass scattering efficiency over North America using a chemical transport model. *Atmospheric Chemistry and Physics*, *19*(4), 2635–2653. https://doi.org/10.5194/acp-19-2635-2019

Li, W., Shao, L., Shi, Z., Chen, J., Yang, L., Yuan, Q., et al. (2014). Mixing state and hygroscopicity of dust and haze particles before leaving Asian continent. *Journal of Geophysical Research: Atmospheres*, *119*(2), 1044–1059. https://doi.org/10.1002/2013JD021003

Lide, D. R. (1995). *CRC handbook of chemistry and physics: A ready-reference book of chemical and physical data*. CRC press.

Linke, C., Möhler, O., Veres, A., Mohácsi, A., Bozóki, Z., Szabó, G., & Schnaiter, M. (2006). Optical properties and mineralogical composition of different Saharan mineral dust samples: A laboratory study. *Atmospheric Chemistry and Physics*, *6*(11), 3315–3323. https://doi.org/10.5194/acp-6-3315-2006

Liu, X. (2022). Dust composition dataset compiled from literature [Dataset]. Mendeley Data. https://doi.org/10.17632/55vd6p28gk.1

Machette, M. N. (1985). Calcific soils of the Southwestern United States. In *Soils and quaternary geology of the Southwestern United States* (Vol. 203, pp. 1–21). Geological Society of America Special Paper.

Macias, E. S., & Hopke, P. K. (Eds.) (1981). *Atmospheric aerosol: Source/Air quality relationships* (Vol. 167). American Chemical Society. https://doi.org/10.1021/bk-1981-0167

Mahowald, N., Jickells, T. D., Baker, A. R., Artaxo, P., Benitez-Nelson, C. R., Bergametti, G., et al. (2008). Global distribution of atmospheric phosphorus sources, concentrations and deposition rates, and anthropogenic impacts. *Global Biogeochemical Cycles*, *22*(4), GB4026. https://doi.org/10.1029/2008GB003240

Mahowald, N. M., Kloster, S., Engelstaedter, S., Moore, J. K., Mukhopadhyay, S., McConnell, J. R., et al. (2010). Observed 20th century desert dust variability: Impact on climate and biogeochemistry. *Atmospheric Chemistry and Physics*, *10*(22), 10875–10893. https://doi.org/10.5194/acp-10-10875-2010

Malm, W. C., & Hand, J. L. (2007). An examination of the physical and optical properties of aerosols collected in the IMPROVE program. *Atmospheric Environment*, *41*(16), 3407–3427. https://doi.org/10.1016/j.atmosenv.2006.12.012

Malm, W. C., Sisler, J. F., Huffman, D., Eldred, R. A., & Cahill, T. A. (1994). Spatial and seasonal trends in particle concentration and optical extinction in the United States. *Journal of Geophysical Research*, *99*(D1), 1347. https://doi.org/10.1029/93JD02916

Manders, A. M. M., Schaap, M., Querol, X., Albert, M. F. M. A., Vercauteren, J., Kuhlbusch, T. A. J., & Hoogerbrugge, R. (2010). Sea salt concentrations across the European continent. *Atmospheric Environment*, *44*(20), 2434–2442. https://doi.org/10.1016/j.atmosenv.2010.03.028

Mason, B. (1952). Principles of geochemistry. *Soil Science*, *74*(3), 262. https://doi.org/10.1097/00010694-195209000-00020

Matassoni, L., Pratesi, G., Centioli, D., Cadoni, F., Malesani, P., Caricchia, A. M., & di Bucchianico, A. D. M. (2009). Saharan dust episodes in Italy: Influence on PM10 daily limit value (DLV) exceedances and the related synoptic. *Journal of Environmental Monitoring*, *11*(9), 1586. https://doi.org/10.1039/b903822a

Matawle, J. L., Pervez, S., Dewangan, S., Shrivastava, A., Tiwari, S., Pant, P., et al. (2015). Characterization of PM2.5 source profiles for traffic and dust sources in Raipur, India. *Aerosol and Air Quality Research*, *15*(7), 2537–2548. https://doi.org/10.4209/aaqr.2015.04.0222

Mendez, J., Guieu, C., & Adkins, J. (2010). Atmospheric input of manganese and iron to the ocean: Seawater dissolution experiments with Saharan and North American dusts. *Marine Chemistry*, *120*(1–4), 34–43. https://doi.org/10.1016/j.marchem.2008.08.006

Meng, J., Martin, R. V., Ginoux, P., Hammer, M., Sulprizio, M. P., Ridley, D. A., & van Donkelaar, A. (2021). Grid-independent high-resolution dust emissions (v1.0) for chemical transport models: Application to GEOS-Chem (12.5.0). *Geoscientific Model Development*, *14*(7), 4249–4260. https://doi.org/10.5194/gmd-14-4249-2021

Miller, R. L., & Tegen, I. (1998). Climate response to soil dust aerosols. *Journal of Climate*, *11*(12), 3247–3267. https://doi.org/10.1175/1520-0442(1998)011<3247:crtsda>2.0.co;2

Møberg, J. P., Esu, I. E., & Malgwi, W. B. (1991). Characteristics and constituent composition of Harmattan dust falling in Northern Nigeria. *Geoderma*, *48*(1–2), 73–81. https://doi.org/10.1016/0016-7061(91)90007-G

Modaihsh, A. S. (1997). Characteristics and composition of the falling dust sediments on Riyadh city, Saudi Arabia. *Journal of Arid Environments*, *36*(2), 211–223. https://doi.org/10.1006/jare.1996.0225

Moreno, T., Amato, F., Querol, X., Alastuey, A., Elvira, J., & Gibbons, W. (2009). Bedrock controls on the mineralogy and chemistry of PM10 extracted from Australian desert sediments. *Environmental Geology*, *57*(2), 411–420. https://doi.org/10.1007/s00254-008-1312-2

Moreno, T., Querol, X., Castillo, S., Alastuey, A., Cuevas, E., Herrmann, L., et al. (2006). Geochemical variations in Aeolian mineral particles from the Sahara–Sahel Dust Corridor. *Chemosphere*, *65*(2), 261–270. https://doi.org/10.1016/j.chemosphere.2006.02.052

Mori, I., Nishikawa, M., Tanimura, T., & Quan, H. (2003). Change in size distribution and chemical composition of kosa (Asian dust) aerosol during long-range transport. *Atmospheric Environment*, *37*(30), 4253–4263. https://doi.org/10.1016/S1352-2310(03)00535-1

Moufti, A. M. B. (2013). Mineralogy, geochemistry and possible provenance of desert sand dunes from western Rub'al Khali area, southeastern Saudi Arabia. *International Journal of Basic and Applied Sciences*, *2*(4), 399–407. https://doi.org/10.14419/ijbas.v2i4.1292

Muhs, D. R., Budahn, J. R., Prospero, J. M., Skipp, G., & Herwitz, S. R. (2012). Soil Genesis on the island of Bermuda in the Quaternary: The importance of African dust transport and deposition. *Journal of Geophysical Research*, *117*(F3), F03025. https://doi.org/10.1029/2012JF002366

Najafi, M. S., Khoshakhllagh, F., Zamanzadeh, S. M., Shirazi, M. H., Samadi, M., & Hajikhani, S. (2014). Characteristics of TSP loads during the Middle East springtime dust storm (MESDS) in Western Iran. *Arabian Journal of Geosciences*, *7*(12), 5367–5381. https://doi.org/10.1007/s12517-013-1086-z

Ni, T., Li, P., Han, B., Bai, Z., Ding, X., Wang, Q., et al. (2013). Spatial and temporal variation of chemical composition and mass closure of ambient PM_{10} in Tianjin, China. *Aerosol and Air Quality Research*, *13*(6), 1832–1846. https://doi.org/10.4209/aaqr.2012.10.0283

Nickovic, S., Vukovic, A., Vujadinovic, M., Djurdjevic, V., & Pejanovic, G. (2012). Technical Note: High-resolution mineralogical database of dust-productive soils for atmospheric dust modeling. *Atmospheric Chemistry and Physics*, *12*(2), 845–855. https://doi.org/10.5194/acp-12-845-2012

Nishikawa, M., Hao, Q., & Morita, M. (2000). Preparation and evaluation of certified reference materials for Asian mineral dust. *Global Environmental Research*, *4*, 1037113.

Nishikawa, M., Kanamori, S., Kanamori, N., & Mizoguchi, T. (1991). Kosa aerosol as eolian carrier of anthropogenic material. *Science of the Total Environment*, *107*, 13–27. https://doi.org/10.1016/0048-9697(91)90247-C

Nowak, S., Lafon, S., Caquineau, S., Journet, E., & Laurent, B. (2018). Quantitative study of the mineralogical composition of mineral dust aerosols by X-ray diffraction. *Talanta*, *186*, 133–139. https://doi.org/10.1016/j.talanta.2018.03.059

Orange, D., Gac, J.-Y., & Diallo, M. (1993). *Geochemical assessment of atmospheric deposition including Harmattan dust in continental West Africa* (Vol. 215, pp. 303–312). IAHS Publication.

Pachon, J. E., Weber, R. J., Zhang, X., Mulholland, J. A., & Russell, A. G. (2013). Revising the use of potassium (K) in the source apportionment of PM2.5. *Atmospheric Pollution Research*, *4*(1), 14–21. https://doi.org/10.5094/APR.2013.002

Pant, P., Shukla, A., Kohl, S. D., Chow, J. C., Watson, J. G., & Harrison, R. M. (2015). Characterization of ambient PM2.5 at a pollution hotspot in New Delhi, India and inference of sources. *Atmospheric Environment*, *109*, 178–189. https://doi.org/10.1016/j.atmosenv.2015.02.074

Peng, C., Gu, W., Li, R., Lin, Q., Ma, Q., Jia, S., et al. (2020). Large variations in hygroscopic properties of unconventional mineral dust. *ACS Earth and Space Chemistry*, *4*(10), 1823–1830. https://doi.org/10.1021/acsearthspacechem.0c00219

Perry, K. D., Cahill, T. A., Eldred, R. A., Dutcher, D. D., & Gill, T. E. (1997). Long-range transport of North African dust to the eastern United States. *Journal of Geophysical Research*, *102*(D10), 11225–11238. https://doi.org/10.1029/97JD00260

Pervez, S., Bano, S., Watson, J. G., Chow, J. C., Matawle, J. L., Shrivastava, A., et al. (2018). Source profiles for PM10-2.5 resuspended dust and vehicle exhaust emissions in central India. *Aerosol and Air Quality Research*, *18*(7), 1660–1672. https://doi.org/10.4209/aaqr.2017.08.0259

Pettijohn, F. J. (1975). *Sedimentary rocks* (Vol. 3). Harper & Row.

Philip, S., Martin, R. V., Pierce, J. R., Jimenez, J. L., Zhang, Q., Canagaratna, M. R., et al. (2014). Spatially and seasonally resolved estimate of the ratio of organic mass to organic carbon. *Atmospheric Environment*, *87*, 34–40. https://doi.org/10.1016/j.atmosenv.2013.11.065

Price, J. R., & Velbel, M. A. (2003). Chemical weathering indices applied to weathering profiles developed on heterogeneous felsic metamorphic parent rocks. *Chemical Geology*, *202*(3–4), 397–416. https://doi.org/10.1016/j.chemgeo.2002.11.001

Pryor, S. C., Simpson, R., Guise-Bagley, L., Hoff, R., & Sakiyama, S. (1997). Visibility and aerosol composition in the Fraser Valley during REVEAL. *Journal of the Air & Waste Management Association*, *47*(2), 147–156. https://doi.org/10.1080/10473289.1997.10464432

Radhi, M., Box, M. A., Box, G. P., Mitchell, R. M., Cohen, D. D., Stelcer, E., & Keywood, M. D. (2010a). Optical, physical and chemical characteristics of Australian continental aerosols: Results from a field experiment. *Atmospheric Chemistry and Physics*, *10*(13), 5925–5942. https://doi.org/10.5194/acp-10-5925-2010

Radhi, M., Box, M. A., Box, G. P., Mitchell, R. M., Cohen, D. D., Stelcer, E., & Keywood, M. D. (2010b). Size-resolved mass and chemical properties of dust aerosols from Australia's Lake Eyre Basin. *Atmospheric Environment*, *44*(29), 3519–3528. https://doi.org/10.1016/j.atmosenv.2010.06.016

Reff, A., Bhave, P. V., Simon, H., Pace, T. G., Pouliot, G. A., Mobley, J. D., & Houyoux, M. (2009). Emissions inventory of $PM_{2.5}$ trace elements across the United States. *Environmental Science & Technology*, *43*(15), 5790–5796. https://doi.org/10.1021/es802930x

Reid, E. A. (2003). Characterization of African dust transported to Puerto Rico by individual particle and size segregated bulk analysis. *Journal of Geophysical Research*, *108*(D19), 8591. https://doi.org/10.1029/2002JD002935

Reimann, C., & de Caritat, P. (2012). New soil composition data for Europe and Australia: Demonstrating comparability, identifying continental-scale processes and learning lessons for global geochemical mapping. *Science of the Total Environment*, *416*, 239–252. https://doi.org/10.1016/j.scitotenv.2011.11.019

Sánchez de la Campa, A., García-Salamanca, A., Solano, J., de la Rosa, J., & Ramos, J.-L. (2013). Chemical and microbiological characterization of atmospheric particulate matter during an intense African dust event in southern Spain. *Environmental Science & Technology*, *47*(8), 3630–3638. https://doi.org/10.1021/es3051235

Santacatalina, M., Reche, C., Minguillón, M. C., Escrig, A., Sanfelix, V., Carratalá, A., et al. (2010). Impact of fugitive emissions in ambient PM levels and composition: A case study in Southeast Spain. *Science of the Total Environment*, *408*(21), 4999–5009. https://doi.org/10.1016/j.scitotenv.2010.07.040

Scheuvens, D., Schütz, L., Kandler, K., Ebert, M., & Weinbruch, S. (2013). Bulk composition of northern African dust and its source sediments—A compilation. *Earth-Science Reviews*, *116*, 170–194. https://doi.org/10.1016/j.earscirev.2012.08.005

Shaw, D. M., Cramer, J. J., Higgins, M. D., & Truscott, M. G. (1986). Composition of the Canadian Precambrian shield and the continental crust of the Earth. *Geological Society, London, Special Publications*, *24*(1), 275–282. https://doi.org/10.1144/GSL.SP.1986.024.01.24

Shen, Z., Caquineau, S., Cao, J., Zhang, X., Han, Y., Gaudichet, A., & Gomes, L. (2009). Mineralogical characteristics of soil dust from source regions in northern China. *Particuology*, *7*(6), 507–512. https://doi.org/10.1016/j.partic.2009.10.001

Shen, Z., Sun, J., Cao, J., Zhang, L., Zhang, Q., Lei, Y., et al. (2016). Chemical profiles of urban fugitive dust PM2.5 samples in Northern Chinese cities. *Science of the Total Environment*, *569–570*, 619–626. https://doi.org/10.1016/j.scitotenv.2016.06.156

Shen, Z. X., Cao, J. J., Arimoto, R., Zhang, R. J., Jie, D. M., Liu, S. X., & Zhu, C. S. (2007). Chemical composition and source characterization of spring aerosol over Horqin sand land in northeastern China. *Journal of Geophysical Research*, *112*(D14), D14315. https://doi.org/10.1029/2006JD007991

Sigsgaard, T., Forsberg, B., Annesi-Maesano, I., Blomberg, A., Bølling, A., Boman, C., et al. (2015). Health impacts of anthropogenic biomass burning in the developed world. *European Respiratory Journal*, *46*(6), 1577–1588. https://doi.org/10.1183/13993003.01865-2014

Simon, H., Beck, L., Bhave, P. V., Divita, F., Hsu, Y., Luecken, D., et al. (2010). The development and uses of EPA's SPECIATE database. *Atmospheric Pollution Research*, *1*(4), 196–206. https://doi.org/10.5094/APR.2010.026

Simon, H., Bhave, P. V., Swall, J. L., Frank, N. H., & Malm, W. C. (2011). Determining the spatial and seasonal variability in OM/OC ratios across the US using multiple regression. *Atmospheric Chemistry and Physics*, *11*(6), 2933–2949. https://doi.org/10.5194/acp-11-2933-2011

Smith, D. B., Solano, F., Woodruff, L. G., Cannon, W. F., & Ellefsen, K. J. (2019). Geochemical and mineralogical maps, with interpretation, for soils of the conterminous United States (Report No. 2017–5118). https://doi.org/10.3133/sir20175118

Snider, G., Weagle, C. L., Martin, R. V., van Donkelaar, A., Conrad, K., Cunningham, D., et al. (2015). SPARTAN: A global network to evaluate and enhance satellite-based estimates of ground-level particulate matter for global health applications. *Atmospheric Measurement Techniques*, *8*(1), 505–521. https://doi.org/10.5194/amt-8-505-2015

Snider, G., Weagle, C. L., Murdymootoo, K. K., Ring, A., Ritchie, Y., Stone, E., et al. (2016). Variation in global chemical composition of $PM_{2.5}$: Emerging results from SPARTAN. *Atmospheric Chemistry and Physics*, *16*(15), 9629–9653. https://doi.org/10.5194/acp-16-9629-2016

Sokolik, I. N., Winker, D. M., Bergametti, G., Gillette, D. A., Carmichael, G., Kaufman, Y. J., et al. (2001). Introduction to special section: Outstanding problems in quantifying the radiative impacts of mineral dust. *Journal of Geophysical Research*, *106*(D16), 18015–18027. https://doi.org/10.1029/2000JD900498

Solomon, P. A., Crumpler, D., Flanagan, J. B., Jayanty, R. K. M., Rickman, E. E., & McDade, C. E. (2014). U.S. National $PM_{2.5}$ chemical speciation monitoring networks—CSN and IMPROVE: Description of networks. *Journal of the Air & Waste Management Association*, *64*(12), 1410–1438. https://doi.org/10.1080/10962247.2014.956904

Solomon, P. A., Fall, T., Salmon, L., Cass, G. R., Gray, H. A., & Davidson, A. (1989). Chemical characteristics of PM_{10} aerosols collected in the Los Angeles area. *Journal of the Air Pollution Control Association*, *39*(2), 154–163. https://doi.org/10.1080/08940630.1989.10466515

Stuut, J.-B., Smalley, I., & O'Hara-Dhand, K. (2009). Aeolian dust in Europe: African sources and European deposits. *Quaternary International*, *198*(1–2), 234–245. https://doi.org/10.1016/j.quaint.2008.10.007

Sullivan, R. C., Moore, M. J. K., Petters, M. D., Kreidenweis, S. M., Roberts, G. C., & Prather, K. A. (2009). Effect of chemical mixing state on the hygroscopicity and cloud nucleation properties of calcium mineral dust particles. *Atmospheric Chemistry and Physics*, *9*(10), 3303–3316. https://doi.org/10.5194/acp-9-3303-2009

Ta, W., Xiao, Z., Qu, J., Yang, G., & Wang, T. (2003). Characteristics of dust particles from the desert/Gobi area of northwestern China during dust-storm periods. *Environmental Geology*, *43*(6), 667–679. https://doi.org/10.1007/s00254-002-0673-1

Tang, M., Cziczo, D. J., & Grassian, V. H. (2016). Interactions of water with mineral dust aerosol: Water adsorption, hygroscopicity, cloud condensation, and ice nucleation. *Chemical Reviews*, *116*(7), 4205–4259. https://doi.org/10.1021/acs.chemrev.5b00529

Tang, M., Zhang, H., Gu, W., Gao, J., Jian, X., Shi, G., et al. (2019). Hygroscopic properties of saline mineral dust from different regions in China: Geographical variations, compositional dependence, and atmospheric implications. *Journal of Geophysical Research: Atmospheres*, *124*(20), 10844–10857. https://doi.org/10.1029/2019JD031128

Taylor, H. E., & Lichte, F. E. (1980). Chemical composition of Mount St. Helens volcanic ash. *Geophysical Research Letters*, *7*(11), 949–952. https://doi.org/10.1029/GL007i011p00949

Taylor, S. R., & McLennan, S. M. (1995). The geochemical evolution of the continental crust. *Reviews of Geophysics*, *33*(2), 241. https://doi.org/10.1029/95RG00262

Tegen, I. (2003). Modeling the mineral dust aerosol cycle in the climate system. *Quaternary Science Reviews*, *22*(18–19), 1821–1834. https://doi.org/10.1016/S0277-3791(03)00163-X

Terzi, E., Argyropoulos, G., Bougatioti, A., Mihalopoulos, N., Nikolaou, K., & Samara, C. (2010). Chemical composition and mass closure of ambient PM10 at urban sites. *Atmospheric Environment*, *44*(18), 2231–2239. https://doi.org/10.1016/j.atmosenv.2010.02.019

Tong, D. Q., Wang, J. X. L., Gill, T. E., Lei, H., & Wang, B. (2017). Intensified dust storm activity and Valley fever infection in the southwestern United States: Dust and Valley Fever Intensification. *Geophysical Research Letters*, *44*(9), 4304–4312. https://doi.org/10.1002/2017GL073524

Torghabeh, A. K., Pradhan, B., & Jahandari, A. (2020). Assessment of geochemical and sedimentological characteristics of atmospheric dust in Shiraz, southwest Iran. *Geoscience Frontiers*, *11*(3), 783–792. https://doi.org/10.1016/j.gsf.2019.08.004

VanCuren, R. A., & Cahill, T. A. (2002). Asian aerosols in North America: Frequency and concentration of fine dust. *Journal of Geophysical Research*, *107*(D24), 4804. https://doi.org/10.1029/2002JD002204

Wang, Y., Zhang, X., Arimoto, R., Cao, J., & Shen, Z. (2005). Characteristics of carbonate content and carbon and oxygen isotopic composition of northern China soil and dust aerosol and its application to tracing dust sources. *Atmospheric Environment*, *39*(14), 2631–2642. https://doi.org/10.1016/j.atmosenv.2005.01.015

Washington, R., Bouet, C., Cautenet, G., Mackenzie, E., Ashpole, I., Engelstaedter, S., et al. (2009). Dust as a tipping element: The Bodele Depression, Chad. *Proceedings of the National Academy of Sciences of the United States of America*, *106*(49), 20564–20571. https://doi.org/10.1073/pnas.0711850106

Wedepohl, K. H. (1995). The composition of the continental crust. *Geochimica et Cosmochimica Acta*, *59*(7), 1217–1232. https://doi.org/10.1016/0016-7037(95)00038-2

Wu, F., Chow, J. C., An, Z., Watson, J. G., & Cao, J. (2011). Size-Differentiated chemical characteristics of Asian Paleo Dust: Records from Aeolian deposition on Chinese Loess Plateau. *Journal of the Air & Waste Management Association*, *61*(2), 180–189. https://doi.org/10.3155/1047-3289.61.2.180

Xu, J. (2004). Aerosol chemical, physical, and radiative characteristics near a desert source region of northwest China during ACE-Asia. *Journal of Geophysical Research*, *109*(D19), D19S03. https://doi.org/10.1029/2003JD004239

Zarasvandi, A., Carranza, E. J. M., Moore, F., & Rastmanesh, F. (2011). Spatio-temporal occurrences and mineralogical–geochemical characteristics of airborne dusts in Khuzestan Province (southwestern Iran). *Journal of Geochemical Exploration*, *111*(3), 138–151. https://doi.org/10.1016/j.gexplo.2011.04.004

Zhang, L., Li, Q. B., Gu, Y., Liou, K. N., & Meland, B. (2013). Dust vertical profile impact on global radiative forcing estimation using a coupled chemical-transport–radiative-transfer model. *Atmospheric Chemistry and Physics*, *13*(14), 7097–7114. https://doi.org/10.5194/acp-13-7097-2013

Zhang, X., Zhao, L., Tong, D., Wu, G., Dan, M., & Teng, B. (2016). A systematic review of global desert dust and associated human health effects. *Atmosphere*, *7*(12), 158. https://doi.org/10.3390/atmos7120158

Zhang, X. Y., Gong, S., Shen, Z., Mei, F., Xi, X., Liu, L., et al. (2003). Characterization of soil dust aerosol in China and its transport and distribution during 2001 ACE-Asia: 1. Network observations. *Journal of Geophysical Research*, *108*(D9), 4261. https://doi.org/10.1029/2002jd002632

Zhao, P., Feng, Y., Zhu, T., & Wu, J. (2006). Characterizations of resuspended dust in six cities of North China. *Atmospheric Environment*, *40*(30), 5807–5814. https://doi.org/10.1016/j.atmosenv.2006.05.026